Check for updates

Remote Sensing in Ecology and Conservation
Open Access
ZSL

RESEARCH ARTICLE

Wall-to-wall Amazon forest height mapping with Planet NICFI, Aerial LiDAR, and a U-Net regression model

Fabien H. Wagner[1,2], Ricardo Dalagnol[1,2], Griffin Carter[1], Mayumi C. M. Hirye[1,3,4], Shivraj Gill[1], Le Bienfaiteur Sagang Takougoum[1,3], Samuel Favrichon[2,5], Michael Keller[2,6], Jean P. H. B. Ometto[7], Lorena Alves[1,3], Cynthia Creze[1,3], Stephanie P. George-Chacon[1,3], Shuang Li[1], Zhihua Liu[1], Adugna Mullissa[1,3], Yan Yang[1], Erone G. Santos[2], Sarah R. Worden[2], Martin Brandt[1,8], Philippe Ciais[1,9], Stephen C. Hagen[1] & Sassan Saatchi[1,2,3]

[1]CTrees, Pasadena California, 91105, USA
[2]Jet Propulsion Laboratory, California Institute of Technology, 4800 Oak Grove, Pasadena California, 91109, USA
[3]Institute of Environment and Sustainability, University of California, Los Angeles, California, USA
[4]Quapá Lab, Faculty of Architecture and Urbanism, University of São Paulo, 05508080, São Paulo, SP, Brazil
[5]Gamma Remote Sensing Ag, Gumligen, Switzerland
[6]USDA Forest Service, International Institute of Tropical Forestry, Rio Piedras, Puerto Rico, USA
[7]Remote Sensing Division, National Institute for Space Research—INPE, São José dos Campos 12227-010,SP, Brazil
[8]Department of Geosciences and Natural Resource Management, University of Copenhagen, Copenhagen 1350, Denmark
[9]Laboratoire des Sciences du Climat et de l'Environnement, CEA-CNRS-UVSQ, CE Orme des Merisiers, Gif sur Yvette 91190, France

Keywords
Canopy height models, forest structure, high-resolution satellite images, tropical forests

Correspondence
Fabien H. Wagner, CTrees, Pasadena, CA 91105, USA. Tel and Fax: +1 9092356294; E-mail: wagner.h.fabien@gmail.com

Editor: Prof. Mat Disney
Associate Editor: Dr. Adrian Pascual

Received: 21 March 2025; Revised: 12 September 2025; Accepted: 13 October 2025

doi: 10.1002/rse2.70041

Abstract

Tree canopy height is a key indicator of forest biomass, productivity and structure, yet measuring it accurately at regional or larger scales, whether from the ground or remotely, remains challenging. The objective of this study is to generate the first complete canopy height map of the Amazon forest at ~4.78 m resolution using Planet NICFI imagery and deep learning. Specifically, we (i) trained a U-Net regression model with canopy height models (CHMs) derived from tropical airborne LiDAR and their corresponding Planet NICFI images to estimate canopy height, (ii) evaluated the accuracy of our map against existing global products based on Sentinel-2/1 and Maxar Vivid2 imagery and (iii) assessed its capacity to capture small-scale canopy height changes. Tree height predictions on the validation sample had a mean absolute error of 3.68 m, with minimal systematic bias across the full range of tree heights in the Amazon forest. The main biases are a slight overestimation (up to 5 m) for heights of 5–15 m and an underestimation for most trees above 50 m. Outperforming existing global model-based canopy height products in this region, the model accurately estimated canopy heights up to 40–50 m with minimal saturation. We determined that the Amazon forest has an average canopy height of ~22 m (standard deviation ~5.3 m) and exhibits large-scale patterns, ranging from the tallest forests of the Guiana Shield to shorter forests along wetlands, rivers, rocky outcrops, savannas and high elevations. Events such as logging or deforestation could be detected from changes in tree height, and the results demonstrated a first success in monitoring the height of regenerating forests. Finally, the map of the Amazon forest canopy height is displayed.

Introduction

The Amazon forest is the most biologically diverse area on the planet, containing around 20% of the diversity of vascular plants, with the number of tree species alone estimated at around 16 000 species (Ter Steege et al., 2013; Zapata-Ríos et al., 2022). In terms of area, the Amazon forest represents > 50% of the world's

© 2025 The Author(s). *Remote Sensing in Ecology and Conservation* published by John Wiley & Sons Ltd on behalf of Zoological Society of London. This is an open access article under the terms of the Creative Commons Attribution-NonCommercial License, which permits use, distribution and reproduction in any medium, provided the original work is properly cited and is not used for commercial purposes.

remaining tropical rainforests, and much of it is still botanically intact (Hansen et al., 2013; Hubbell et al., 2008). The Amazon forest biomass constitutes one of the largest terrestrial carbon pools in the world, estimated at ~ 150–200 GtC (Lv et al., 2021; Mo et al., 2023). While still functioning as a carbon sink, this role is increasingly challenged by disturbances (Pan et al., 2024; Rosan et al., 2024). Recently, the Amazon rainforest has experienced significant changes in tree cover and forest structure due to extensive deforestation (National Institute for Space Research (INPE), Earth Observation General Coordination, 2024; de Almeida et al., 2021), degradation from logging and fire (Bourgoin et al., 2024; Lapola et al., 2023; Matricardi et al., 2020; Qin et al., 2021), and increased drought and extreme conditions (da Silva et al., 2023; Gloor et al., 2013; Marengo & Espinoza, 2016). Some forest areas are regenerating after deforestation, but accurately estimating this regrowth and its sink potential remains in its early stages (Bastin et al., 2019; Heinrich et al., 2021; Heinrich et al., 2023; Mo et al., 2023; Silva Junior et al., 2020). To protect this ecosystem, support policies to limit deforestation, improve timber-harvesting practices and identify potential areas for forest restoration requires better forest structure and biomass estimation at individual tree level (Mo et al., 2023; Pan et al., 2024). While these metrics can be derived from canopy height (Asner & Mascaro, 2014; Lim et al., 2003; Longo et al., 2016), an Essential Biodiversity Variable (Skidmore et al., 2021), domain-scale estimation of tree height remains challenging.

Airborne LiDAR provides the most accurate forest canopy height estimates, but its high cost limits coverage to small or sparse areas. In the Brazilian Amazon, significant efforts have been made to flight airborne LiDAR and capture forest structure diversity through scientifically based LiDAR sampling design and over permanent plots with field measurements (Csillik et al., 2024; Dos-Santos et al., 2022; Ometto et al., 2023). The GEDI (Dubayah et al., 2020; Liu et al., 2025) and ICESat (Lefsky, 2010; Lefsky et al., 2005; Markus et al., 2017) missions provide additional Amazon coverage, but their observations are sparse and have coarser resolution than airborne LiDAR. Current approaches use machine/deep learning with multispectral and radar imagery, trained on LiDAR or GEDI reference data, to estimate tree height over larger areas. These models can infer canopy height from local to global scales using various data sources, including Landsat (Potapov et al., 2021), Sentinel-2 (Astola et al., 2021; Lang et al., 2019; Lang et al., 2023), combined Sentinel-1/2 imagery (Fayad et al., 2023; Ge et al., 2022; Pauls et al., 2024; Schwartz et al., 2023; Schwartz et al., 2024), Planet imagery (Csillik et al., 2019; Huang et al., 2022; Liu et al., 2023), very high-resolution (VHR) airborne data (Karatsiolis et al., 2021; Li et al., 2020; Li et al., 2023; Wagner et al., 2024) and Maxar satellite VHR images (Illarionova et al., 2022; Tolan et al., 2024).

Global canopy height models (CHMs) typically use Landsat or Sentinel-1/2 (Lang et al., 2023; Pauls et al., 2024; Potapov et al., 2021), but their spatial resolutions (30 m or 10 m) are too coarse to identify individual trees. Maxar Vivid2 commercial imagery is also used by Meta (Tolan et al., 2024), but it suffers from heterogeneity due to system properties and data collection strategy, and incompleteness in the Amazon due to clouds. The complete high-resolution CHM for the Amazon is still to be done. Planet NICFI images (Planet Team, 2017) currently provide the best data for Amazon monitoring, offering 4.78 m spatial resolution multispectral data (RGB + NIR) between 30° N and 30° S. Monthly cloud-free composites are created from the best daily acquisitions of the month. Despite limited radiometric accuracy (Pooja et al., 2021), Planet data have been used successfully to map tree cover (Carter et al., 2024; Wagner et al., 2023) and forest degradation (CTrees.org, 2024; Dalagnol et al., 2023) in the Amazon. Planet NICFI is currently the only dataset that enables consistent temporal monitoring of canopy structure in the Amazon at less than 10 m spatial resolution and represents a unique resource for advancing Amazon canopy height mapping.

Examples of regional or larger-scale canopy height mapping with deep learning are rare in the tropics and typically come from global datasets (Lang et al., 2023; Pauls et al., 2024; Tolan et al., 2024), while such methods are slightly more developed in other regions, such as boreal and temperate forests (Astola et al., 2021; Fayad et al., 2023; Illarionova et al., 2022; Li et al., 2023; Liu et al., 2023; Schwartz et al., 2023, 2024; Wagner et al., 2024). With the exception of Tolan's model (Tolan et al., 2024), which uses a fine-tuned foundation model, most other studies demonstrate that tree height estimation can be achieved with great accuracy using encoder-decoder deep learning architectures trained locally (Rolf et al., 2024), such as U-Net (Ronneberger et al., 2015). This highlights locally trained U-Nets as the architecture of choice for mapping canopy height in the Amazon.

The objective of this study is to generate the first complete canopy height map of the Amazon at ~ 4.78 m resolution using Planet NICFI imagery and deep learning. Specifically, we aim to (i) demonstrate that U-Net architectures trained with CHMs derived from tropical airborne LiDAR, together with their time-aligned Planet NICFI images, can provide reliable canopy height estimates at ~ 4.78 m resolution, (ii) evaluate the performance of our map against existing global products, including those from Sentinel-2 and -1 (10 m) and Maxar

© 2025 The Author(s). *Remote Sensing in Ecology and Conservation* published by John Wiley & Sons Ltd on behalf of Zoological Society of London.

20563485, 0, Downloaded from https://zslpublications.onlinelibrary.wiley.com/doi/10.1002/rse2.70041, Wiley Online Library on [01/03/2026]. See the Terms and Conditions (https://onlinelibrary.wiley.com/terms-and-conditions) on Wiley Online Library for rules of use; OA articles are governed by the applicable Creative Commons License

Vivid2 mosaic imagery (0.5 m) and (iii) assess its ability to detect small-scale changes in canopy height resulting from deforestation, logging and regeneration. Finally, we present the Amazon forest tree height map for the 2020–2024 period.

Methods

Data

Planet NICFI satellite images

To train the model and predict the tree canopy height of the Amazon forest, we used Planet satellite images from NICFI (https://www.nicfi.no/) (Planet Team, 2017) at 4.78 m resolution. Approximately, 1 240 000 images covering the Amazon (8 260 920 km^2, Fig. 1) were downloaded through Planet API, with biannual coverage (2015–2020, 10 dates) and monthly coverage (2020–2024, 46 dates). The Planet NICFI images are distributed in tiles of size 4096 × 4096 pixels (~20 × 20 km), and in the following text, *tile* refers to the Planet NICFI tile. The 12-bit Red (0.650–0.682 m), Green (0.547–0.585 m), Blue (0.464–0.517 m), and NIR (0.846–0.888 m) bands were first scaled 0–2540 (RGB truncated to 0–2540 and NIR divided by 3.937), scaled to 8-bit (0–255), and combined into RGBNIR composites without atmospheric correction.

LiDAR airborne datasets

The Embrapa LiDAR datasets were collected under the "Sustainable Landscapes – Brazil" Program to assess carbon stocks and human impacts in the Amazon Forest (Dos-Santos et al., 2022). LiDAR data were acquired across Amazon, Cerrado, and Atlantic Forest from 2008 to 2018, with ongoing collection (https://www.paisagenslidar.cnptia.embrapa.br/). We only kept LiDAR data collected in 2015 or later to overlap with the Planet NICFI dates. The publicly available LAZ files have ~10 points/m^2 resolution and each covers 1 km^2. We used 1149 LAZ files of 70 flights from 23 Brazilian sites (2015–2018) and 1 Peruvian site (2017).

The EBA project collected LiDAR transects across the Brazilian Amazon (2016–2018) (Ometto et al., 2023), available at https://zenodo.org/records/7636454. Each

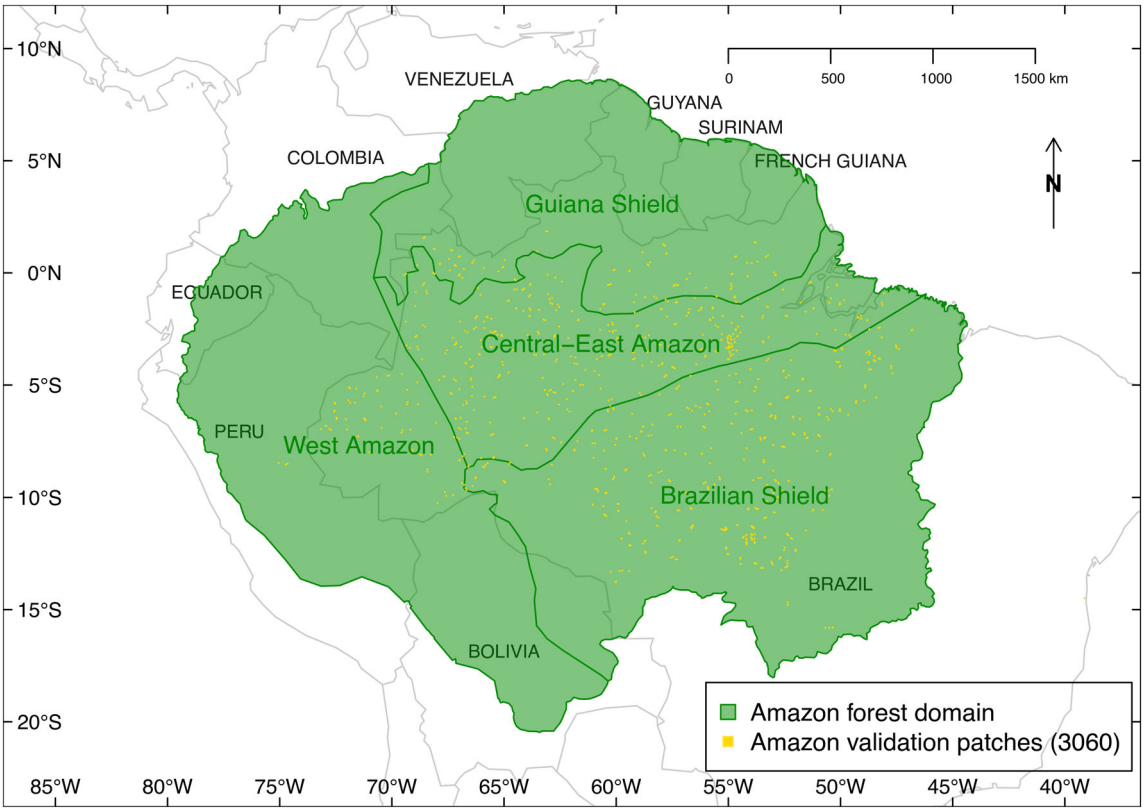

Figure 1. Extent of the Amazon forest domain used in this study and its partition into four regions according to Feldpausch et al. (2011). The location of the 3060 validation patches of 256 × 256 pixels in the Amazon domain is shown in gold. The validation locations approximately represent the locations of all LiDAR flights in the Amazon used in the study, as at least one patch per flight was used for validation. The additional 376 validation patches in the Atlantic Forest domain, mostly located over São Paulo city, are not displayed on the map.

© 2025 The Author(s). *Remote Sensing in Ecology and Conservation* published by John Wiley & Sons Ltd on behalf of Zoological Society of London.

20563485, 0, Downloaded from https://zslpublications.onlinelibrary.wiley.com/doi/10.1002/rse2.70041, Wiley Online Library on [01/03/2026]. See the Terms and Conditions (https://onlinelibrary.wiley.com/terms-and-conditions) on Wiley Online Library for rules of use; OA articles are governed by the applicable Creative Commons License

Transect (713 total) covered 375 hectares minimum using a Trimble Harrier 68i sensor with 4 returns/m^2, 30° field of view, and 600 m flight height. Data accuracy was <1 m horizontal and <0.5 m vertical. We used 19 302 LAZ files ($\sim 1000 \times 1000$ m each).

The São Paulo Metropolitan Region dataset was collected in 2017 and is available at https://registry.opendata.aws/pmsp-lidar/. These data were used to train the model on diverse backgrounds (pasture, soil, buildings) and Atlantic Forest areas. The survey used an Optech Gemini sensor with 100–125 KHz frequency, 18–25° scan angle, 0.25 mrad beam divergence, 700 m flight height and 8 returns/m^2 density. We used 5554 LAZ files (500 × 500 m each).

LiDAR point clouds (.LAZ format) were processed into CHMs using the LidR R package (Roussel et al., 2020; Roussel & Auty, 2021). First, outliers in the LiDAR point clouds were eliminated through denoising using the *ivf* algorithm, with a resolution set to 1 m and a maximum of 5 surrounding points (Roussel & Auty, 2021). Second, the point cloud was classified using the progressive morphological filter (pmf) algorithm with parameters ws = seq(4, 42, 3), or ws = seq(3, 12, 3) if the algorithm had difficulty converging, and th = seq(0.1, 1.5, length.out = length(ws)). Third, the digital terrain model (DTM) and digital surface model (DSM) were generated at a spatial resolution of 1 m. The *TIN* algorithm (Roussel & Auty, 2021) was applied to compute the DTM, while the DSM was generated using the *pitfree* algorithm with thresholds set to [0, 2, 5, 10, 15] and a maximum edge length of [0, 1.5]. All the parameters were chosen to produce a smooth 1 m CHM without any holes reaching the ground inside the crowns, which can occur with other parameterizations and could impede a good fit of the U-Net model, as the model focuses on these large, unpredictable errors. The final CHM was created by subtracting DTM from DSM, scaling by 2.5 and converting to 8-bit integer format to optimize height resolution within the 0–255 range.

Building footprints masking

Google's Building Footprints for South America (https://sites.research.google/open-buildings/) was used to remove building heights from CHM. Building polygons were buffered (5 m outside cities, 15 m inside) and rasterized to match CHM resolution. All CHM pixels intersecting these buffered footprints were set to zero.

Global tree height datasets

We evaluated our model against three deep learning-based global canopy height datasets: Meta's 0.5 m resolution map using DINOv2 and Maxar RGB imagery (Meta and World Resources Institute (WRI), 2023; Tolan et al., 2024), Lang's 10 m resolution map using CNN and Sentinel-2 data (Lang et al., 2023), and Paul's 10 m resolution map using CNN with Sentinel-1/2 data (Pauls et al., 2024). All used GEDI or aerial LiDAR as reference data.

Deforestation and logging datasets

To analyze tree canopy height changes, we used two Planet NICFI-based datasets: a deforestation dataset showing monthly tree cover changes (CTrees.org, 2024; Wagner et al., 2023) and a logging dataset showing biannual activities (CTrees.org, 2024; Dalagnol et al., 2023) in pan-tropical evergreen forests. These datasets were used to find areas of deforestation, regeneration and selective logging in the Amazon and their dates of occurrence.

Model

Neural Network Architecture

We used a U-Net model (Ronneberger et al., 2015) to estimate Amazon forest canopy height from Planet NICFI images, Figure 2. The model processes 256 × 256 pixel RGB-NIR inputs (4.78 m resolution) to produce height predictions at pixel level. Implementation used R with Keras and TensorFlow 2.10 (Abadi et al., 2015; Allaire & Chollet, 2016; Allaire & Tang, 2020; Chollet, 2015; R Core Team, 2016).

Training and validation

To generate samples for model training and validation, for a given LiDAR flight, we selected all Planet NICFI tiles that overlapped its extent and were closest in date to the flight. Then, to increase sample size and reduce cloud effects, we also included Planet NICFI images from adjacent dates, assuming no significant forest height change within up to 1 year. This corresponds to ±6 months for the biannual Planet NICFI time series. The 1 m CHM data were resampled to 4.78 m Planet resolution using median values, along with a binary mask indicating CHM data presence. The median was used to minimize the impact of outliers in the 1 m CHM. Both Planet images and resampled CHM data (4096 × 4096 pixels) were split into 256 × 256 patches using gdal_retile (GDAL/OGR contributors, 2019). To maximize the use of the LiDAR dataset and ensure independent validation, we selected a 256×256 sub-image for validation from each Planet tile intersecting the flight lines, with the remaining data used for training. The validation data came from the same

© 2025 The Author(s). *Remote Sensing in Ecology and Conservation* published by John Wiley & Sons Ltd on behalf of Zoological Society of London.

20563485, 0, Downloaded from https://zslpublications.onlinelibrary.wiley.com/doi/10.1002/rse2.70041, Wiley Online Library on [01/03/2026]. See the Terms and Conditions (https://onlinelibrary.wiley.com/terms-and-conditions) on Wiley Online Library for rules of use; OA articles are governed by the applicable Creative Commons License

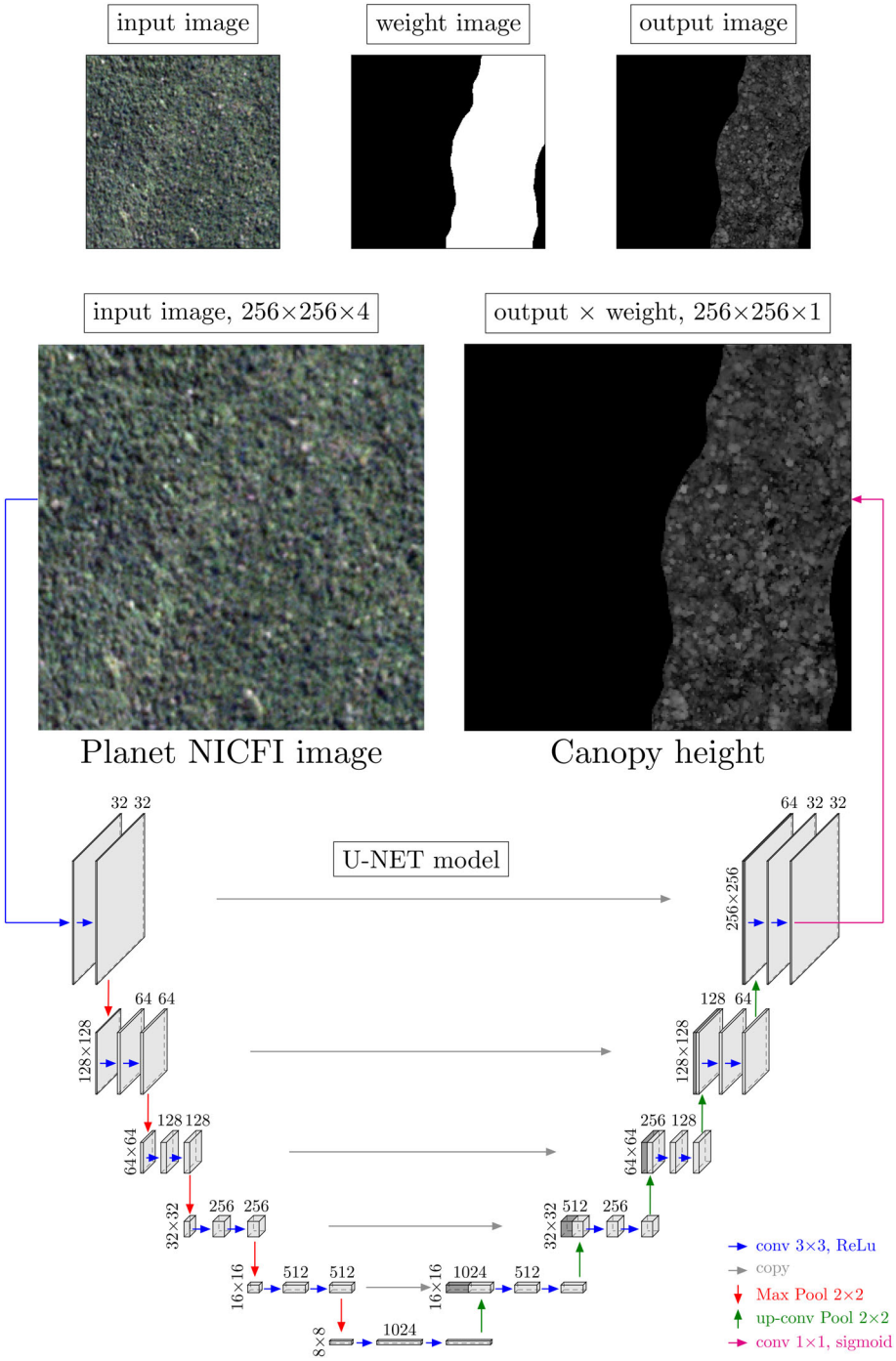

Figure 2. U-Net architecture used to estimate canopy height from Planet NICFI imagery, adapted from Ronneberger et al. (2015). The number of channels is shown above each cuboid, and the vertical dimensions represent the row and column sizes in pixels. Operations such as convolutions, skip connections, max pooling and upsampling, along with their respective sizes, are illustrated with colored arrows. For the weight, the white area (value = 1) corresponds to pixels with CHM data, while the black area (value = 0) represents NA values.

flights as the training data but did not spatially overlap with the training samples. The dataset included 50 724 patches of 256 × 256 pixels (47 288 training, 3436 validation), with validation patches distributed randomly along the flight lines across Amazon (3060, as shown in Fig. 1) and Atlantic (376) forests.

© 2025 The Author(s). *Remote Sensing in Ecology and Conservation* published by John Wiley & Sons Ltd on behalf of Zoological Society of London.

20563485, 0, Downloaded from https://zslpublications.onlinelibrary.wiley.com/doi/10.1002/rse2.70041, Wiley Online Library on [01/03/2026]. See the Terms and Conditions (https://onlinelibrary.wiley.com/terms-and-conditions) on Wiley Online Library for rules of use; OA articles are governed by the applicable Creative Commons License

The U-Net model was trained using SGD optimization with the Adam optimizer (learning rate 0.0001), weighted mean squared error loss, horizontal and vertical flips for data augmentation and 1000 epochs with 32-image batches. The best model achieved 0.0008285521 validation loss and 3.62 m mean absolute error, training in under 24 h on an Nvidia RTX4090 GPU.

For the 3436 validation images, we assessed the accuracy of the predicted canopy heights at the pixel level using the root mean square error (RMSE), the mean absolute error (MAE), the Bias, along with their percentages relative to the mean reference canopy height, RMSE %, MAE% and Bias%, Equations (1–7). All accuracy metrics were also computed using the three global canopy height datasets on the validation images to enable comparison with our results.

$$\overline{H}_{\text{ref}} = \frac{1}{N}\sum_{i=1}^{N} H_{\text{ref},i} \tag{1}$$

$$RMSE = \sqrt{\frac{1}{N}\sum_{i=1}^{N}\left(H_{\text{pred},i} - H_{\text{ref},i}\right)^2} \tag{2}$$

$$RMSE\% = \frac{RMSE}{\overline{H}_{\text{ref}}} \times 100 \tag{3}$$

$$MAE = \frac{1}{N}\sum_{i=1}^{N}\left|H_{\text{pred},i} - H_{\text{ref},i}\right| \tag{4}$$

$$MAE\% = \frac{MAE}{\overline{H}_{\text{ref}}} \times 100 \tag{5}$$

$$Bias = \frac{1}{N}\sum_{i=1}^{N}\left(H_{\text{pred},i} - H_{\text{ref},i}\right) \tag{6}$$

$$Bias\% = \frac{Bias}{\overline{H}_{\text{ref}}} \times 100 \tag{7}$$

where N = number of validation samples, $H_{pred,i}$ = predicted canopy height at pixel i, $H_{ref,i}$ = reference canopy height at pixel i.

Finally, median and percentiles (0.05–0.95) of canopy height were computed within each validation area to summarize the canopy height distribution and to provide complementary insight into model performance across the distribution of observed values.

Amazon Forest 2020–2024 Canopy Height Map Production

For prediction, NICFI tiles were padded to 4224 × 4224 with adjacent tiles pixels values, then trimmed by 64 pixels to reduce border artifacts (Ronneberger et al., 2015). Mean Amazon forest height (2020–2024) was calculated at pixel level from observations between 2016 and 2024, excluding clouds, cloud shade and areas deforested before 2020 or regenerated after 2020 (CTrees.org, 2024; Wagner et al., 2023). Pixels with forest loss between 2020 and 2024 were retained in the analysis which may lower mean canopy height mainly near Amazon forest edges where deforestation occurred. Cloud shade in the monthly height mask appears as continuous areas with very high values that do not correspond to real forest structure. We generate a cloud shade mask to identify and remove these false high-value areas as follows. First, we apply thresholding to create a binary mask of pixels with height values greater than 32 m. Next, we apply erosion using a 16 × 16 kernel to eliminate isolated high pixels, such as single crowns or noise. Then, we apply dilation with a 512 × 512 kernel to expand the remaining high-value areas. Finally, we use the resulting mask to exclude cloud shade pixels from the mean height computation. If no valid values for a pixel are available across the entire time series, which occurs only in regions of extreme shading or in areas with very tall trees, we gradually increase the threshold to 36 m and, if necessary, to 40 m. For the forested pixels, height ≥5 m following the definition of FAO (2020), we computed the mean canopy height using the mean height per tile and the number of valid tree height observations per tile as weights, Equation (8), where i is a Planet tile, and a valid observation is a pixel with tree height ≥ 5 m and more than 5 non-cloud observations. The weighted percentiles 2.5, 5, 25, 50, 75, 95 and 97.5 over the Amazon were also computed using the same per-tile logic. In "Valid Observations in Planet NICFI Data" "Amazon Forest Canopy Height" and "Comparison with Global Canopy Height Products" sections, we use the Planet NICFI tile as the unit for computing and displaying descriptive statistics.

$$\text{Weighted mean} = \frac{\sum_{i=1}^{n}(\text{Mean}_i \times \text{Valid observations}_i)}{\sum_{i=1}^{n}\text{Valid observations}_i} \tag{8}$$

Results

Accuracy and comparison with global CHM models

Our model accurately predicted canopy height, with predictions closely following the 1:1 line across 3436 validation patches (Fig. 3A). The accuracy metrics are ranked consistently with the MAE, Table 1, with our model showing the best performance, followed by Tolan's model, Pauls's model and Lang's model. Specifically, our model showed an MAE of 3.68 m (MAE% = 25.87%), an RMSE of 5.54 m (RMSE% = 38.91%) and Bias of −0.28 m (Bias % = −1.97%). The predicted height is within 1 m, 3 m and 5 m of the reference in 33.9%, 55.6% and 71.6% of

© 2025 The Author(s). *Remote Sensing in Ecology and Conservation* published by John Wiley & Sons Ltd on behalf of Zoological Society of London.

20563485, 0, Downloaded from https://zslpublications.onlinelibrary.wiley.com/doi/10.1002/rse2.70041, Wiley Online Library on [01/03/2026]. See the Terms and Conditions (https://onlinelibrary.wiley.com/terms-and-conditions) on Wiley Online Library for rules of use; OA articles are governed by the applicable Creative Commons License

cases, respectively. The model performs well up to 45–50 m but underestimates taller trees, though trees above 50 m represent only 0.06% of validation pixels. While accurate for non-forest areas, it slightly overestimates heights below 25 m. Note that Planet and CHM images are not co-registered, and NICFI basemaps combine images with varying dates, sensor calibrations, illuminations or acquisition geometries.

Tolan's 0.5 m Maxar-based model (Tolan et al., 2024) shows good accuracy (MAE: 4.7 m) but saturates at 30–35 m and exhibits cloud-related zero height errors (Fig. 3B). Like our model, it overestimates heights below 25 m. Pauls's 10 m Sentinel-1/2-based model (Pauls et al., 2024) has 6.9 m MAE and saturates at 40 m (Fig. 3C). It overestimates low vegetation height with minimum predictions of 2–3 m. Lang's 10 m Sentinel-2-based model (Lang et al., 2023) reaches 40–45 m with 8.14 m MAE (Fig. 3D). Despite overestimation due to 10 m resolution and training methodology favoring taller canopies, it effectively captures tall trees.

Table 1. Accuracy metrics for the validation dataset for our canopy height model and the three global models of Tolan, Pauls and Lang. MAE, RMSE and Bias are reported, along with their percentages relative to the mean reference canopy height.

	Our model	Tolan's model	Pauls's model	Lang's model
MAE (m)	3.68	4.70	6.90	8.14
MAE% (%)	25.87	33.05	48.47	57.20
RMSE (m)	5.54	7.23	8.31	10.57
RMSE% (%)	38.91	50.82	58.36	74.28
Bias (m)	−0.28	−2.30	3.54	7.41
Bias% (%)	−1.97	−16.16	24.85	52.10

Predicted height distribution analysis

Observed validation data show a bimodal height distribution with peaks at zero and ∼20 m (Fig. 4A). Our model closely matches this pattern and predicts heights more uniformly than other models (Fig. 4B), though slightly

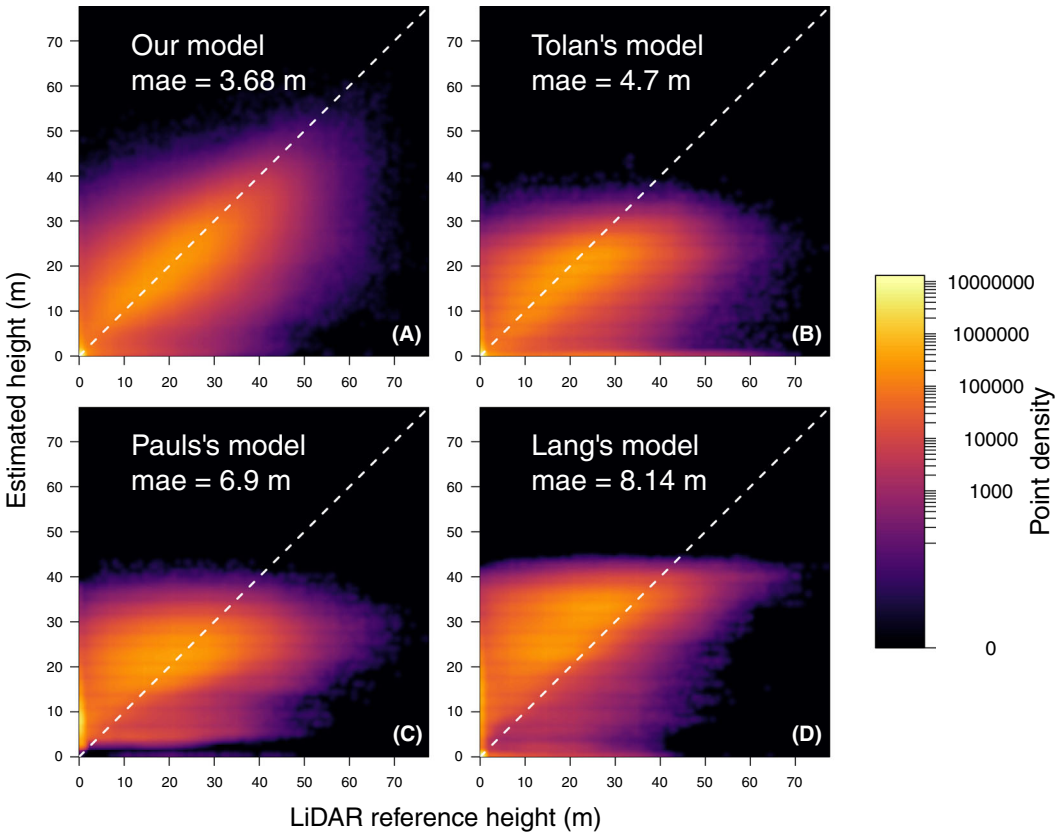

Figure 3. Comparison of predicted versus observed height (m) for the 3436 validation patches represented as density scatterplots for our CHM (A), Tolan's model (B) and Lang's model (C). Tolan's model and Lang's model, with native spatial resolutions of 0.5 m and 10 m respectively, were warped to our 4.78 m spatial resolution using the median and nearest neighbor algorithms, respectively. Each plot contains c. 63 million points. The 1:1 line and the MAE are depicted in white.

© 2025 The Author(s). *Remote Sensing in Ecology and Conservation* published by John Wiley & Sons Ltd on behalf of Zoological Society of London.

20563485, 0, Downloaded from https://zslpublications.onlinelibrary.wiley.com/doi/10.1002/rse2.70041, Wiley Online Library on [01/03/2026]. See the Terms and Conditions (https://onlinelibrary.wiley.com/terms-and-conditions) on Wiley Online Library for rules of use; OA articles are governed by the applicable Creative Commons License

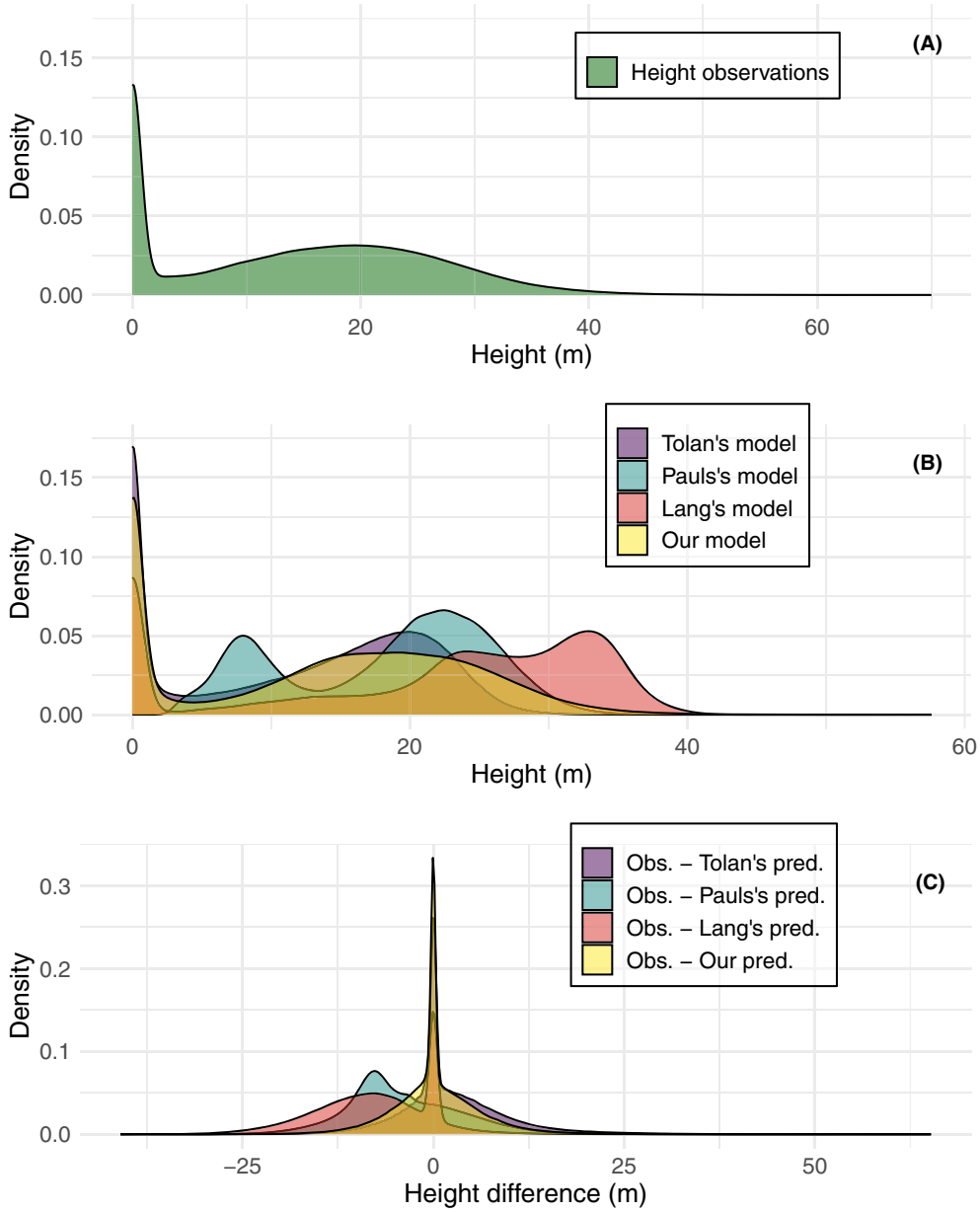

Figure 4. Distribution of observed height in the validation sample (A); predicted height distribution for our model, Tolan's, Pauls's and Lang's models (B); and differences in predicted height between our model and the others (C). Tolan's, Pauls's and Lang's models (native resolutions: 0.5 m, 10 m and 10 m) were warped to our 4.78 m resolution using median or nearest neighbor algorithms.

underestimating above 20 m and overestimating below. Tolan's model shows a narrow distribution peaking at 20 m, underestimating taller heights, with more instances of zero height than observed, likely due to cloud cover. Pauls's model exhibits peaks at 22–23 m and 5–10 m, overestimating canopy and low vegetation heights with no near-zero values. Lang's model shows three peaks (near-zero, 24 m and 33 m), generally overestimating heights.

Height difference distributions (Fig. 4C) show our model performs best, with Tolan's and Lang's models also peaking at zero. Our predictions are uniformly distributed around zero, while Tolan's model shows excess positive differences due to underestimation above 20–30 m. Both Paul's and Lang's models exhibit negative difference distributions, indicating systematic height overestimation.

© 2025 The Author(s). *Remote Sensing in Ecology and Conservation* published by John Wiley & Sons Ltd on behalf of Zoological Society of London.

20563485, 0, Downloaded from https://zslpublications.onlinelibrary.wiley.com/doi/10.1002/rse2.70041, Wiley Online Library on [01/03/2026]. See the Terms and Conditions (https://onlinelibrary.wiley.com/terms-and-conditions) on Wiley Online Library for rules of use; OA articles are governed by the applicable Creative Commons License

Example of predictions from the models

Our model effectively reproduces crown-level CHM across different forest structures (Fig. 5). In dense, tall forests (Fig. 5A–E), we clearly identify crowns despite some height underestimation, while Tolan's model appears blurrier, Pauls's model captures large crowns but struggles with lower points, and Lang's model identifies tree groups well. In uniform dense forests (Fig. 5F–J), our model maintains crown detection, while Tolan's model only captures large trees, Pauls's underestimates tall trees and Lang's shows cloud-related data gaps. For lower density forests (Fig. 5K–O), we capture crowns but miss gaps, Tolan's appears blurry, Pauls's matches our heights but is blurrier, and Lang's follows overall canopy structure. In forests with isolated large crowns (Fig. 5P–T), our model is the best at crown and gap detection, Tolan's captures large crowns and gaps well, Pauls's overestimates low canopy but detects large crowns and Lang's captures tall tree groups but overestimates overall. In uniform low forests (Fig. 5U–Y), we provide the best resolution but may miss lower points that Tolan's captures, while Pauls's overestimates heights except for large crowns, and Lang's captures spatial patterns despite overestimation.

In forests with a smooth and large canopy height transitions (Fig. 6A–E), our model and Tolan's achieve good resolution and low heights, while Pauls's and Lang's models overestimate heights. For rivers inside forests (Fig. 6F–J), our model and Tolan's correctly map water as zero height, Pauls's only detects larger rivers, and Lang's sometimes misinterprets rivers as tall vegetation. At forest-clear-cut boundaries (Fig. 6K–O), our model captures borders and isolated trees well, Tolan's appears blurrier, while Pauls's and Lang's fail to reach zero in cleared areas. In smooth height transitions (Fig. 6P–T), all models perform well, though Tolan's shows cloud artifacts. For small gaps and roads (Fig. 6U–Y), Tolan's model detects low points, while our model struggles, and Pauls's and Lang's miss these fine-scale features, though

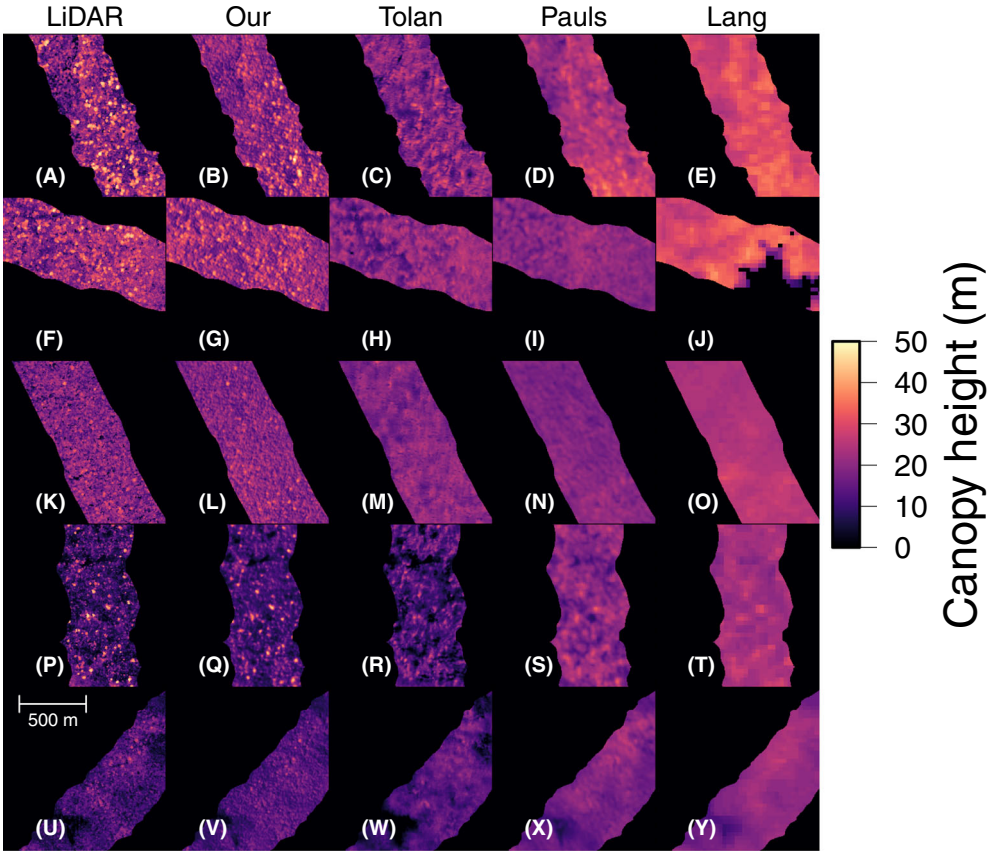

Figure 5. Example of canopy height models observed in the validation dataset (column 1), predicted from our model (column 2), Tolan's model (column 3) and Lang's model (column 4). Tolan's, Pauls's and Lang's models (native resolutions: 0.5 m, 10 m and 10 m) were warped to our 4.78 m resolution using the median or nearest neighbor algorithms. Image centroids per row in decimal latitude and longitude: [−7.411495, −53.552856]; [−0.2142329, −62.7154541]; [−11.82972, −53.95935]; [−7.182651, −51.597290]; and [−9.941798, −52.739868].

© 2025 The Author(s). *Remote Sensing in Ecology and Conservation* published by John Wiley & Sons Ltd on behalf of Zoological Society of London.

20563485, 0, Downloaded from https://zslpublications.onlinelibrary.wiley.com/doi/10.1002/rse2.70041, Wiley Online Library on [01/03/2026]. See the Terms and Conditions (https://onlinelibrary.wiley.com/terms-and-conditions) on Wiley Online Library for rules of use; OA articles are governed by the applicable Creative Commons License

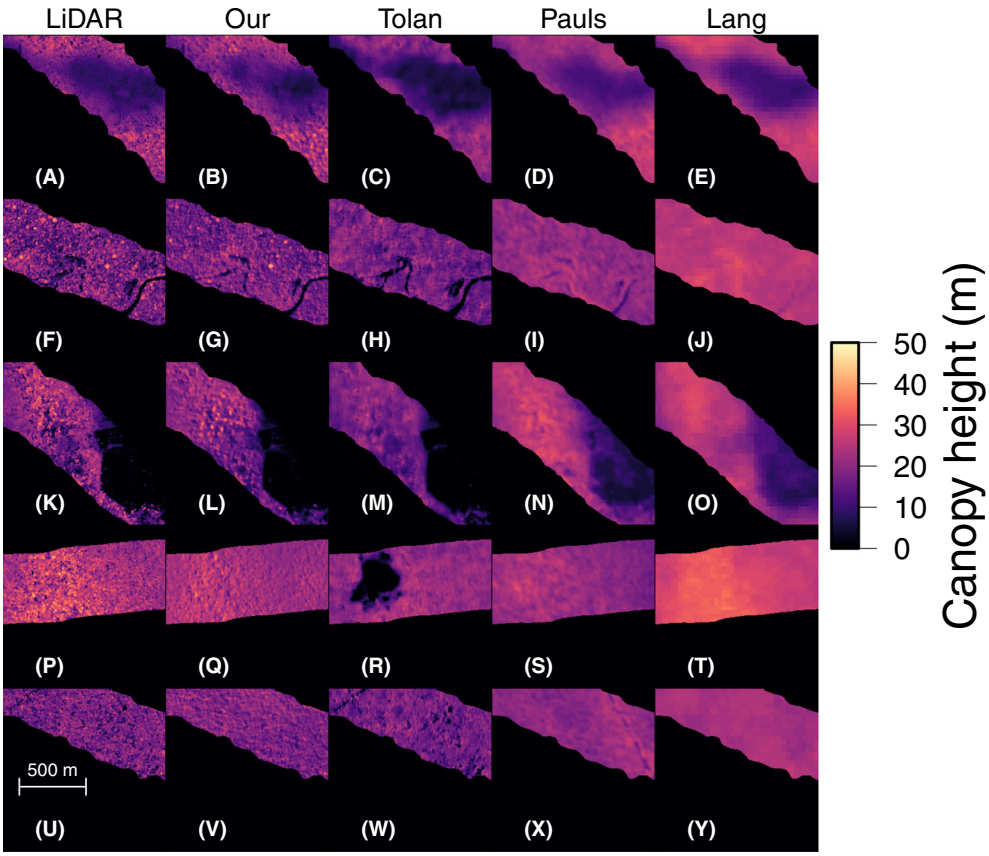

Figure 6. Example of canopy height models observed in the validation dataset (column 1), predicted from our model (column 2), Tolan's model (column 3) and Lang's model (column 4). Tolan's, Paul's and Lang's models (native resolutions: 0.5 m, 10 m and 10 m) were warped to our 4.78 m resolution using the median or nearest neighbor algorithms. Image centroids per row in decimal latitude and longitude: [−10.47161, −56.68396]; [−6.320758, −50.938110]; [−10.50402, −56.64001]; [−4.778995, −61.814575]; and [−10.48241, −53.77258].

Pauls's captures newer roads (built after our validation sample image was taken in 2018).

Height distribution at validation patch-level from our model

Across the 3436 validation patches (Fig. 7A), the 5th percentile shows high correlation with LiDAR reference but overestimates heights above 1–2 m, especially at 5–15 m. The median (50th percentile, Fig. 7B) demonstrates best accuracy ($\rho = 0.927$) with predictions well-distributed along the 1:1 line. The 95th percentile (Fig. 7C) shows increasing underestimation with height (−5 to −10 m for tallest trees), possibly because taller trees don't necessarily have proportionally larger crowns.

Logging detection from height changes

In a Mato Grosso selective logging site (Fig. 8), activities were tracked through 2022. The site was selected based on disturbance model results from Dalagnol et al. (2023) because it experienced successive logging events close in time, with minimal cloud cover, allowing clear visual assessment of these events. Between March and April (Fig. 8A,B), new logging appeared below center and top-right, visible in RGB images and height difference maps despite illumination and geolocation noise (Fig. 8C). From April to May (Fig. 8D,E), logging moved above center, with clear canopy height reductions (Fig. 8F). During June–July (Fig. 8G,H), activity concentrated below center, with marked height reductions (Fig. 8I). Despite some noise in the raw model output, large removed trees appear to show up in the canopy height differences between dates, suggesting the potential for detecting logging events at the tree level.

Clear-cut and regeneration detection from canopy height changes

Figure 9 shows the height time series for deforestation and regrowth. Point 1 maintained stable height (2016–2019) before deforestation and has a sharp decrease

© 2025 The Author(s). *Remote Sensing in Ecology and Conservation* published by John Wiley & Sons Ltd on behalf of Zoological Society of London.

20563485, 0, Downloaded from https://zslpublications.onlinelibrary.wiley.com/doi/10.1002/rse2.70041, Wiley Online Library on [01/03/2026]. See the Terms and Conditions (https://onlinelibrary.wiley.com/terms-and-conditions) on Wiley Online Library for rules of use; OA articles are governed by the applicable Creative Commons License

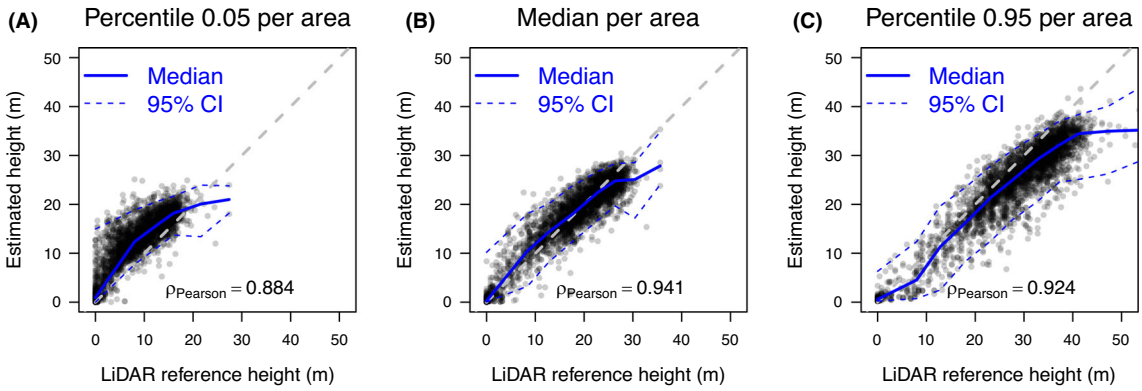

Figure 7. Percentile 0.05 (A), median (B) and percentile 0.95 (C) of heights computed from canopy heights observed and predicted by our model in the 3436 validation patches. Median of the points and 95% confidence interval computed by intervals of 5 m is given in blue. Each point represents one validation patch.

in height in 2020, confirmed by our deforestation algorithm (CTrees.org, 2024; Wagner et al., 2023), with minimal subsequent regrowth. Point 2 showed stability until late 2018's deforestation, and Point 3's deforestation occurred mid-2017, both showing little regrowth. Points 4 and 5 demonstrate regrowth after deforestation in 2020, detected by our algorithm. Point 6, initially non-forest in 2015, shows continuous regrowth from 2018 to 2019, reaching 15–20 m by 2024. All time series show height variations due to cloud effects (Fig. 9).

Artifacts from clouds and shade

Raw predictions show various artifacts from clouds, haze, shade and blur (Fig. 10). The model handles light haze well, maintaining crown visibility (location 1, Fig. 10A,B), but underestimates heights in blurred areas (location 2). Cloud presence reduces heights to zero, masking canopy features (location 3), while shaded forests show height overestimation (location 4). Our cloud mask enables us to discard all errors caused by clouds; for example, the entire image in Figure 10A is classified as cloudy.

Valid observations in Planet NICFI data

The Planet time series used in this study comprised 56 dates: 10 biannual basemaps (2015-12-01 to 2020-06-01) and 46 monthly basemaps (2020-09-01 to 2024-06-01). Thus, each pixel could have up to 56 valid (i.e., cloud-free) observations. In the following text, the number of observations is aggregated by NICFI tile to facilitate comparison between regions. Of 22 063 Amazon NICFI tiles, 8.06% (1860) had pixels lacking observations, though those tiles also had pixels with at least three observations. From 56 possible dates, tiles averaged 32.34 cloud-free observations, varying geographically (Fig. 11). Southern Amazon showed the highest coverage (up to 55.9 observations), while the lowest counts occurred in French Guiana (0.25, quad *0717–1048*), Guiana Shield, western Amazon near Andes and central-western Amazon boundary. For low-observation regions, we made the cloud/shade masking less restrictive to increase valid observations (Amazon Forest 2020–2024 Canopy Height Map Production section).

Amazon forest canopy height

We found that the mean canopy height of the Amazon forest was 22.09 m, with a standard deviation of 5.270 m, a median of 22.25 m and a 97.5th percentile of 32.10 m (Table 2).

Highest mean canopy heights (Fig. 12a) concentrate in the Eastern Guiana Shield and upper West Amazon/Central-East Amazon border, with Guiana Shield containing most continuous regions reaching ∼30 m. The 97.5th percentile height distribution (Fig. 12b) forms a 1000 km-wide circle around Central Amazon, exceeding 50 m in some areas. Notable tall forest hotspots include the French Guiana-Brazil border, areas south of the Amazon River (∼500 km from Atlantic) and western Amazon region. On the western slopes of the Andes, there seem to be no natural forests, only tree plantations; the values (mean and 97.5th) represent only the few plantations within the 20 × 20 km tiles.

Lower canopy heights occur in several distinct regions: (i) near the Amazon River and wetlands, including Peru's Marañón Basin and Bolivia's Llanos de Mojos savannas; (ii) along Andean elevation gradients near treeline; (iii) around rocky outcrops, such as the Tepuis in Venezuela;

© 2025 The Author(s). *Remote Sensing in Ecology and Conservation* published by John Wiley & Sons Ltd on behalf of Zoological Society of London.

20563485, 0, Downloaded from https://zslpublications.onlinelibrary.wiley.com/doi/10.1002/rse2.70041, Wiley Online Library on [01/03/2026]. See the Terms and Conditions (https://onlinelibrary.wiley.com/terms-and-conditions) on Wiley Online Library for rules of use; OA articles are governed by the applicable Creative Commons License

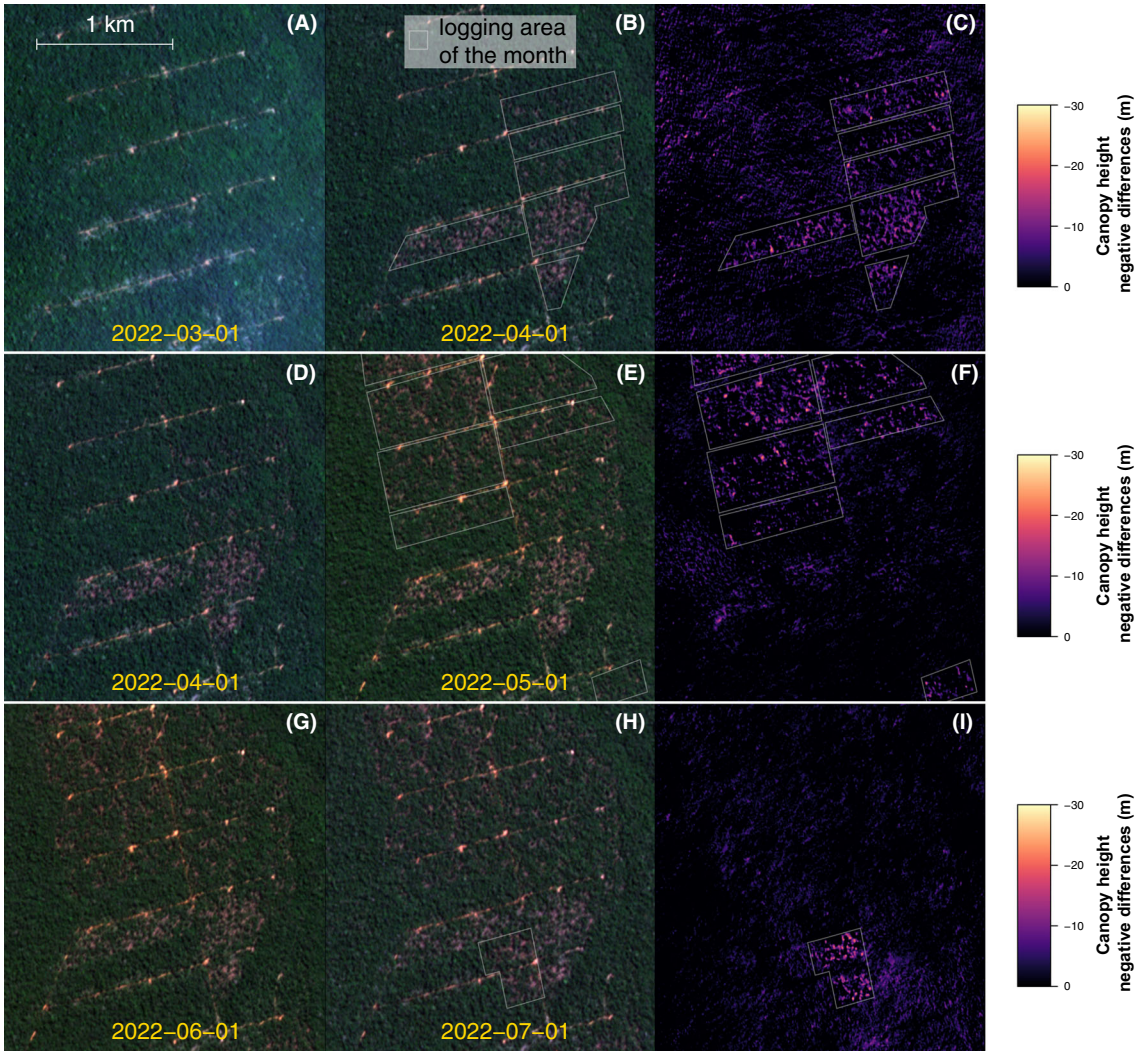

Figure 8. Examples of height changes due to selective logging activities for the Planet quad 0714–0954 for the periods 2022-03-01 to 2022-04-01 (A–C), 2022-04-01 to 2022-05-01 (D–F) and 2022-06-01 to 2022-07-01 (G–I). Each row of images corresponds to one of these periods and includes: a color composite image of the area (left), a color composite image of the subsequent month showing logging activity (middle), and a canopy height difference map (right). The image size is c. 2.45 km × 2.45 km. Image centroid in decimal latitude and longitude [−12.15929, −54.46710].

(iv) in savanna ecosystems, where the lowest canopy height is at the Brazil-Guyana-Venezuela borders; and (v) near deforested areas and particularly in the Arc of Deforestation.

Comparison with global canopy height products

Compared with Tolan's model (Fig. 13a), our heights are higher (> 10 m) in Guyana shield and western Amazon, confirming Tolan's 30 m saturation (Fig. 3b), though both capture landscape height variations well. Pauls's model shows <10 m differences from ours (Fig. 13b), performing better near Andes due to combined radar-optical data (Pauls et al., 2024), but underestimating fragmented forests in the Arc of deforestation. Lang's mean RH98 exceeds our mean heights in dense canopy areas but is lower in sparse forests (Fig. 13c). Their RH98 versus our 97.5th percentile shows higher values in Guiana Shield and Andes, possibly due to better optical data coverage and geographic variables, but underestimates heights in fragmented forests (Fig. 13d).

Overall, our model provides higher height estimates across Amazon, except in high cloud/shade regions near the Andes, while maintaining good spatial agreement with other models despite different data sources.

© 2025 The Author(s). *Remote Sensing in Ecology and Conservation* published by John Wiley & Sons Ltd on behalf of Zoological Society of London.

20563485, 0, Downloaded from https://zslpublications.onlinelibrary.wiley.com/doi/10.1002/rse2.70041, Wiley Online Library on [01/03/2026]. See the Terms and Conditions (https://onlinelibrary.wiley.com/terms-and-conditions) on Wiley Online Library for rules of use; OA articles are governed by the applicable Creative Commons License

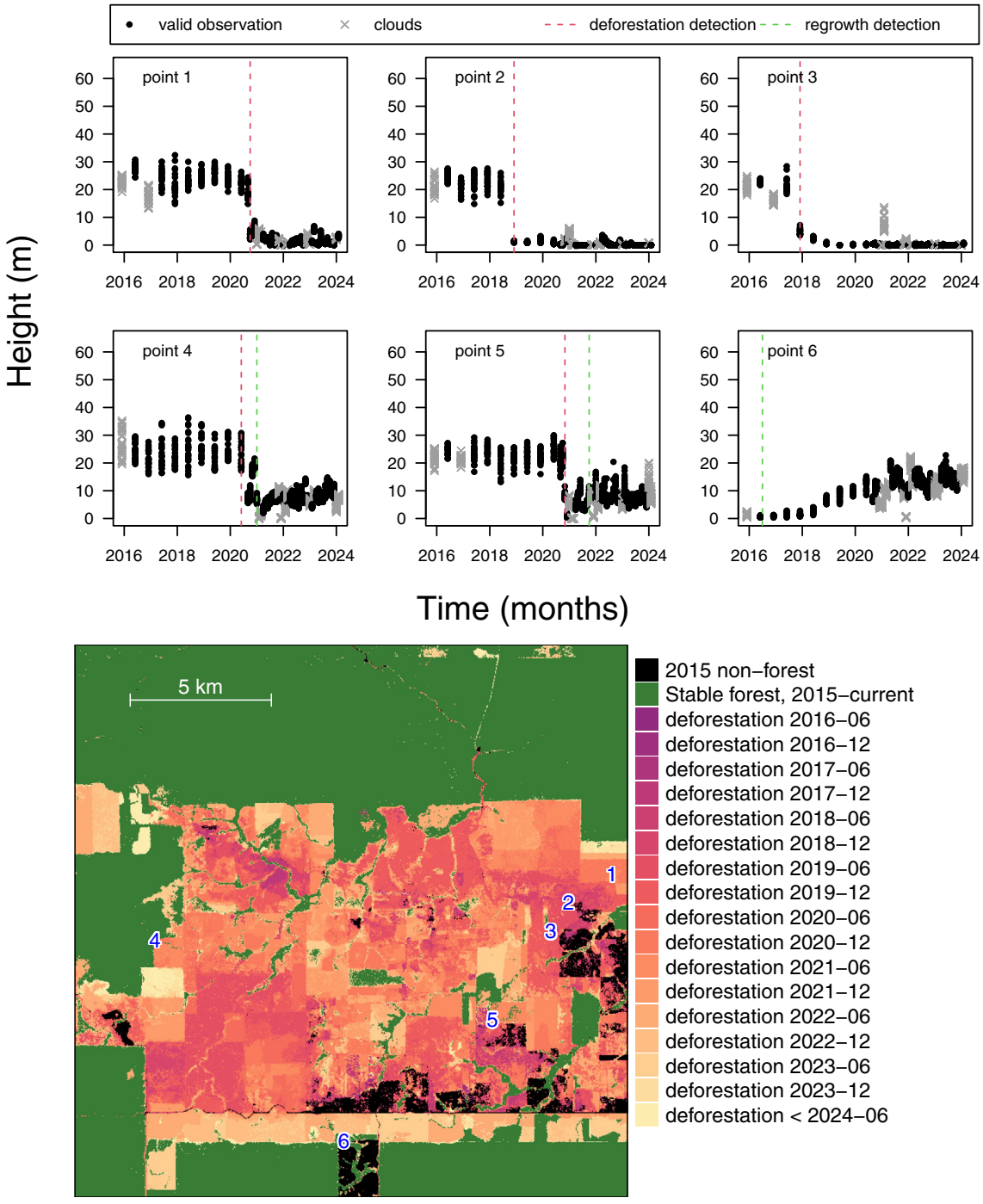

Figure 9. Example of height time series in case of deforestation (points 1, 2 and 3), deforestation and regrowth (points 4, 5) and only regrowth (points 6). For each location, the value of the point and its 24 closest neighbors are presented. To reduce the effect of possible geolocation errors between dates, we considered the neighboring pixels to assess the mean temporal behavior of an area rather than individual pixels. The locations of these points are displayed on our previously developed Planet NICFI-based deforestation product for the Planet quad 0681–0967 spanning from December 1, 2015, to February 1, 2024. The Planet NICFI quad covers approximately 19.5 × 19.5 km. Tile centroid in decimal latitude and longitude [−9.882275, −60.205078].

© 2025 The Author(s). *Remote Sensing in Ecology and Conservation* published by John Wiley & Sons Ltd on behalf of Zoological Society of London.

20563485, 0, Downloaded from https://zslpublications.onlinelibrary.wiley.com/doi/10.1002/rse2.70041, Wiley Online Library on [01/03/2026]. See the Terms and Conditions (https://onlinelibrary.wiley.com/terms-and-conditions) on Wiley Online Library for rules of use; OA articles are governed by the applicable Creative Commons License

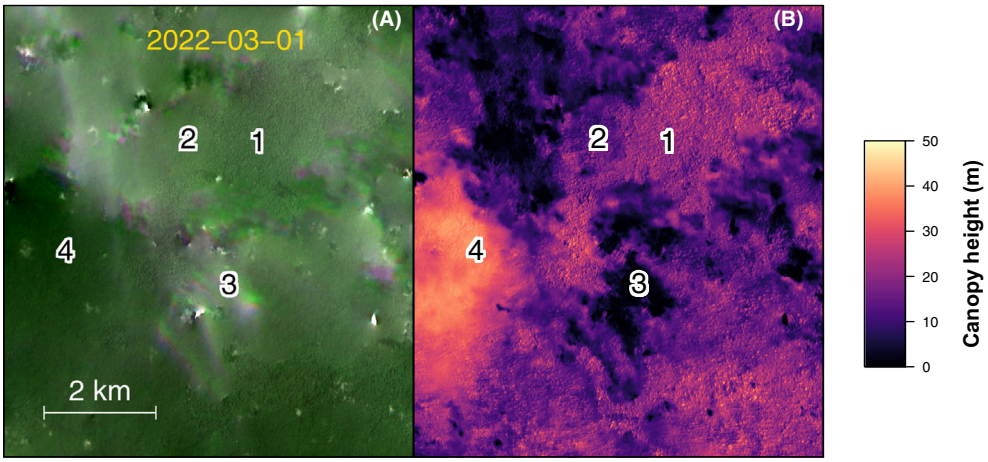

Figure 10. Example of artifacts in height prediction caused by haze, blur, clouds and shade in the NICFI images before cloud correction for the Planet quad 0722–1038 basemap of 2022-03-01. Location 1 is a hazy but clear part of the image for reference, location 2 is a blurry part of the image, location 3 is a cloudy area with very high reflectance values, and location 4 is a shaded part of the image. Note that this image is classified as 100% clouds after filtering by our cloud model. The image size is ~7.34 × 7.34 km. Image centroid in decimal latitude and longitude [2.602864, −52.943115].

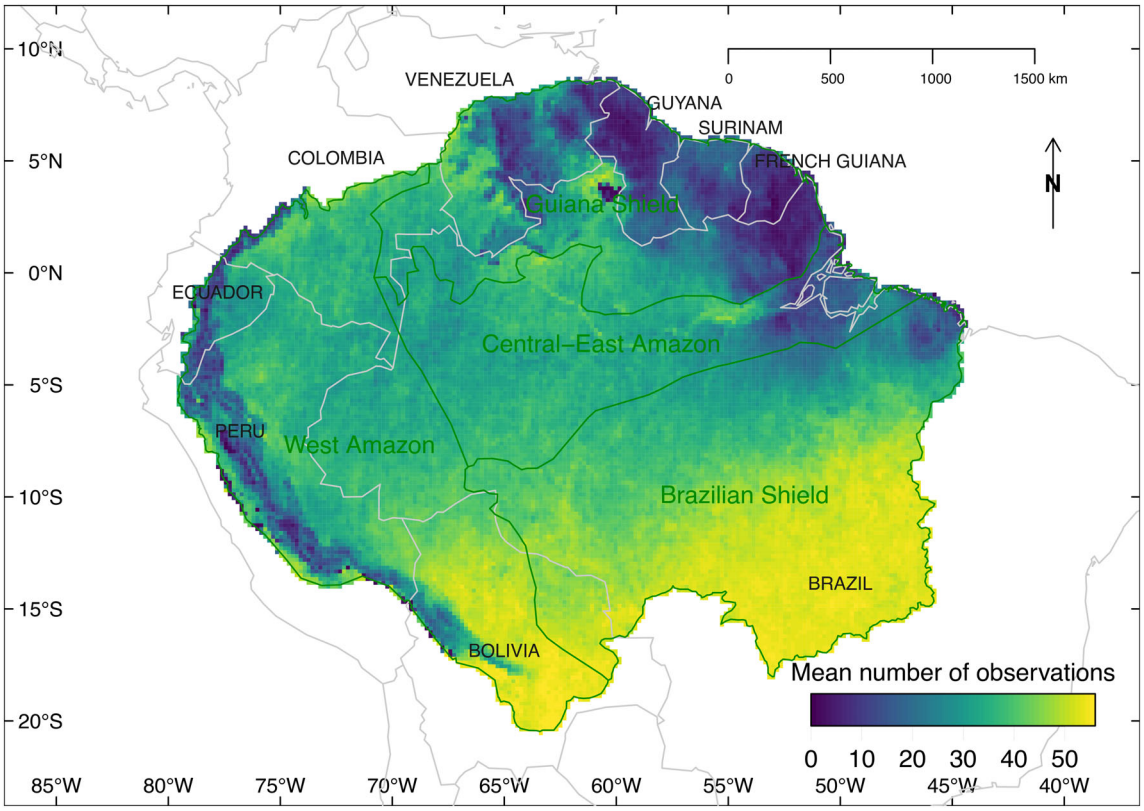

Figure 11. Mean number of cloud-free observations for the ~20 km × 20 km pixels corresponding to the Planet NICFI tiles. Only pixels with vegetation height greater than zero were considered in the mean computation. The maximum number of observations is 56, corresponding to the 56 NICFI mosaic dates.

© 2025 The Author(s). *Remote Sensing in Ecology and Conservation* published by John Wiley & Sons Ltd on behalf of Zoological Society of London.

20563485, 0, Downloaded from https://zslpublications.onlinelibrary.wiley.com/doi/10.1002/rse2.70041, Wiley Online Library on [01/03/2026]. See the Terms and Conditions (https://onlinelibrary.wiley.com/terms-and-conditions) on Wiley Online Library for rules of use; OA articles are governed by the applicable Creative Commons License

Table 2. Amazon forest canopy height descriptive statistics.

Canopy height Metrics	Value (m)
Mean	22.09
Standard deviation	5.270
Percentile 2.5	11.34
Percentile 5	13.25
Percentile 25	18.75
Median, Percentile 50	22.25
Percentile 75	25.54
Percentile 95	30.54
Percentile 97.5	32.10

High-resolution map of the Amazon canopy height

The VHR canopy height map of the Amazon forest shows highly diverse and consistent large-scale spatial patterns of tree height (Fig. 14). As observed in the analysis (Amazon forest canopy height section), variables associated with lower heights include (i) natural factors, such as wetlands, savannas and rocky outcrops, and (ii) human activities like deforestation and roads. In Brazil, roads are already following the arc of taller forests revealed by the p97.5 canopy height (Fig. 12b), and some large forested areas within this arc have already been deforested and fragmented.

For most of the Amazon forest, the model enables the detection of the tallest trees with the largest crowns, Figure 15. These trees were visually identified by examining groups of pixels above 40 m across some regions of the Amazon. The first individual, Figure 15a–c, has a crown diameter of c. 70 m, making it the largest tree found in our Amazon dataset so far, and likely one of the largest tree crowns in the Amazon forest. All the other trees also have crown diameters above 50 m, which explains their good visibility in the NICFI image with a spatial resolution of 4.78 m. Each of these trees exhibits distinct annual phenology, with a complete renewal of leaves occurring within 1–2months every year during the same period (observed from 2021 to 2024). The species are unknown.

Discussion

Here, we show that Planet NICFI images with a 4.78 m spatial resolution enable accurate mapping of Amazon forest canopy height, even allowing the identification of most large tree crowns. The U-Net network, adapted for regression, estimated canopy height with a mean error of 3.68 m on the validation dataset. This confirms the high capacity of convolutional networks to support vegetation mapping, particularly canopy height mapping with high spatial resolution images (Kattenborn et al., 2021; Wagner et al., 2024). However, since the discontinuation of the Planet NICFI program, both historical and real-time Planet imagery is no longer open access. This will limit the application of the method for academic, non-governmental and governmental organizations due to the cost of commercial data.

We found that the Amazon forest has a mean canopy height of 22.09 m, a median of 22.25 m and a 97.5th percentile of 32.10 m. The tallest forests form a 1000 - km-wide arc around the Central Amazon. A canopy height hotspot was identified in the Guiana Shield, near the southern border of French Guiana and Brazil, where the tallest documented Amazon trees, such as a *Dinizia excelsa* reaching 88.5 m, have been recorded (Gorgens et al., 2019). On the Amazon forest scale, the canopy height varies significantly, with shorter forests near rivers, wetlands, savannas and deforested areas, reflecting local environmental and anthropogenic influences (Fig. 14).

For the Amazon forest, our locally calibrated model provided more accurate canopy height estimates, with a better prediction range and less saturation, than available global models (Figs. 3 and 4). It is the only one that effectively captures tree heights beyond 45 m. While expected for lower resolution models (Lang et al., 2023; Pauls et al., 2024), it also outperformed Tolan's higher-resolution (0.5 m) Maxar-based model (Tolan et al., 2024), suggesting high-quality local training data's importance over resolution (Rolf et al., 2024). Several factors could explain why our height estimates are better. First, the U-Net architecture uses all local information with only minimal compression, whereas other architectures, such as Dino V1 used in Tolan's model, seem to lose fine-scale details due to compression. Second, the $\sim$5 m resolution of our CHM dataset used for training produces smoother crowns, likely making predictions easier than for 1 m CHMs, which may contain significant intra-crown variation, while at larger scales, such as 10 m or 30 m, individual crowns are no longer visible. Finally, the extensive aerial LiDAR training data covering a wide range of heights across Brazilian tropical forests likely contributed, while Tolan's model used only a small portion from the Atlantic Forest, which lacks tall trees. Our canopy height map, Fig. 14, shows similar spatial patterns to other maps (Lang et al., 2023; Pauls et al., 2024; Tolan et al., 2024), but reaches greater heights and provides crown-level detail, enabling temporal monitoring.

Some regions exhibit higher canopy heights, such as the Guiana Shield and the western Amazon (Fig. 12B), but the most prominent patterns of canopy height seem to be influenced by edaphic conditions. Studies in the Amazon have reported that forests on plateaus with

© 2025 The Author(s). *Remote Sensing in Ecology and Conservation* published by John Wiley & Sons Ltd on behalf of Zoological Society of London.

20563485, 0, Downloaded from https://zslpublications.onlinelibrary.wiley.com/doi/10.1002/rse2.70041, Wiley Online Library on [01/03/2026]. See the Terms and Conditions (https://onlinelibrary.wiley.com/terms-and-conditions) on Wiley Online Library for rules of use; OA articles are governed by the applicable Creative Commons License

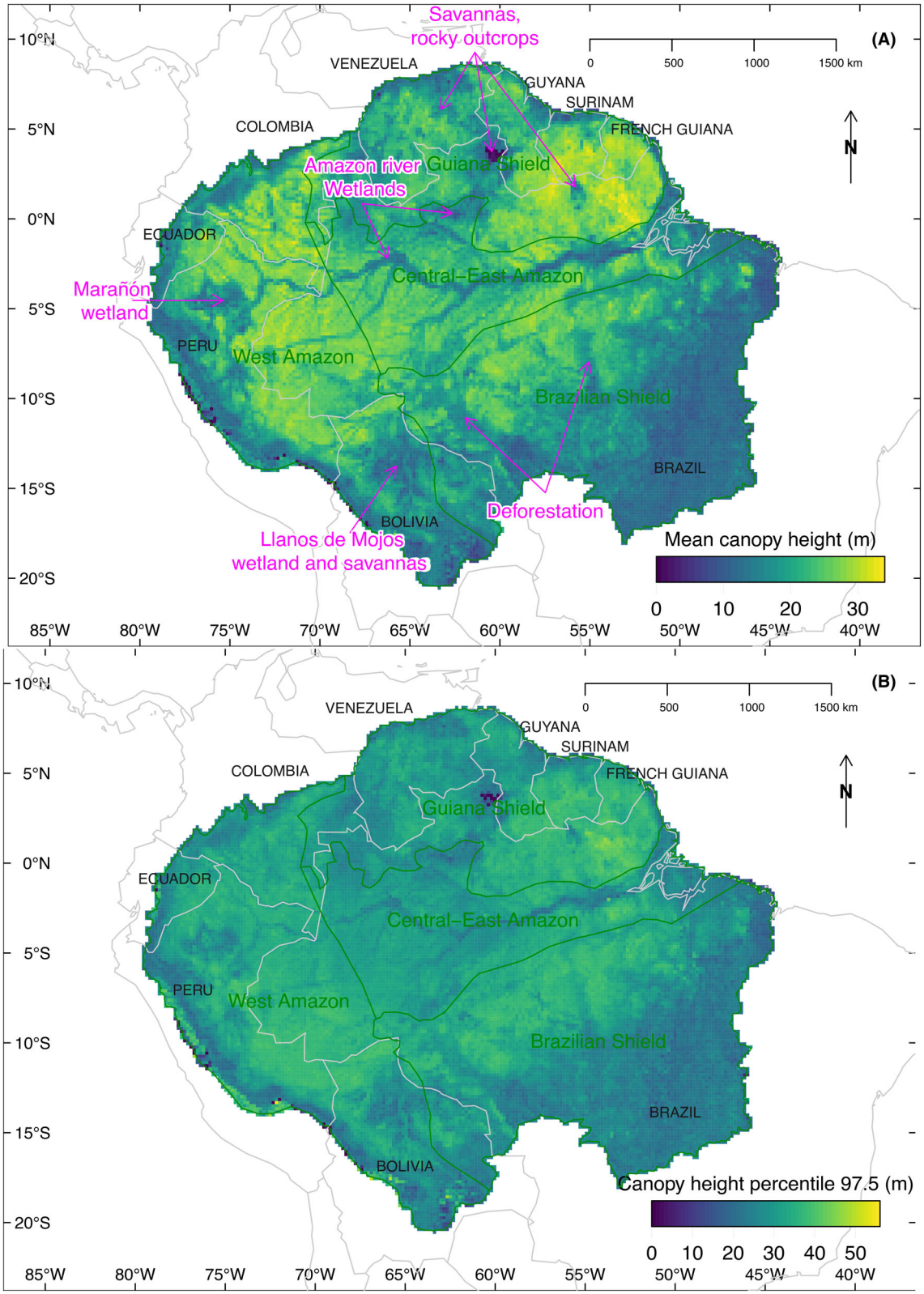

Figure 12. Map of the mean and percentile 97.5th of the Amazon forest tree canopy height on the period 2020–2024 (a–b). Each statistics is given for ~20 km × 20 km pixels which correspond to a planet tile. Inside a tile, mean and percentile 97.5th are computed only with pixels that have ≥ three non-clouded observation.

© 2025 The Author(s). *Remote Sensing in Ecology and Conservation* published by John Wiley & Sons Ltd on behalf of Zoological Society of London.

20563485, 0, Downloaded from https://zslpublications.onlinelibrary.wiley.com/doi/10.1002/rse2.70041, Wiley Online Library on [01/03/2026]. See the Terms and Conditions (https://onlinelibrary.wiley.com/terms-and-conditions) on Wiley Online Library for rules of use; OA articles are governed by the applicable Creative Commons License

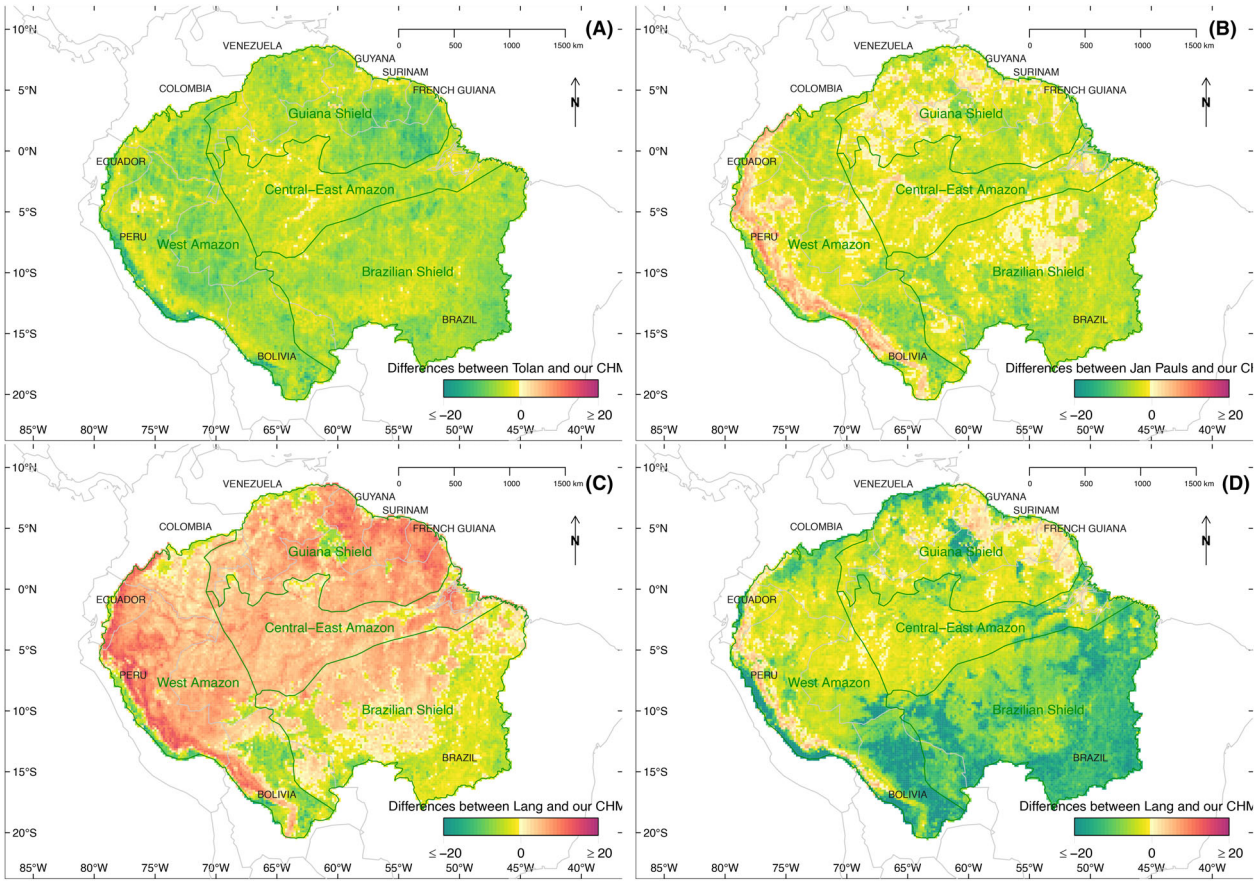

Figure 13. Tree canopy height differences in meters between Tolan's product (a), Pauls's product (b), Lang's product (c–d) and our canopy height product. For Lang's product, we compared it to the mean of our product (c) and the 97.5th percentile (d), as Lang models the GEDI 98% relative height (RH98). Differences are shown for the ~20 km × 20 km Planet NICFI tiles, considering only pixels with vegetation height greater than zero. A negative difference means our canopy height is higher than the compared product.

well-drained clay soils tend to have taller and more uneven canopies compared with forests in areas along rivers, on white-sand soils, or on shallow soils (Feldpausch et al., 2011; Gonçalves et al., 2024; Laurance et al., 1999; Quesada et al., 2012; Rosa et al., 2017). In other words, poorly drained, shallow, or rapidly draining soils tend to support lower biomass and shorter trees. Consistent with these previous findings, our map shows the lowest canopy heights near wetlands, major rivers, high elevations, rocky outcrops and savannas, such as those in southern Guyana and the Roraima region (Figs. 12A and 14). Maximum height appears to represent an upper limit achievable by most Amazon forests, as shown by the 97.5th percentile in Figure 12a, regardless of forest basal area or mean wood density, which are known to increase from the driest to the wettest regions and from the west to the east, respectively (Avitabile et al., 2016; Malhi et al., 2006). Finally, our map highlights large-scale human disturbance effects on Amazon forest height, with visible scars of deforestation in the Brazilian Shield and western Amazon region (Figs. 12A and 14).

The Amazon forest has high spatial variability in species (Luize et al., 2024), forest structure and biomass (de Conto et al., 2024; Saatchi et al., 2011). Our large-scale height patterns reinforce that the Amazon is a highly heterogeneous forest, with notable features like the tall tree hotspot in the Guiana Shield (Gorgens et al., 2019). This heterogeneity raises particular conservation concerns, as deforestation in the Amazon still targets large continuous forest patches, Figure 14, and removes unique forest ecosystems.

Our map may underestimate Andean canopy heights due to cloud cover and shading, where radar-based models like Pauls' are more reliable (Lang et al., 2023; Pauls et al., 2024). While we used strict cloud masking with 1200 m buffers to ensure very high-quality, cloud-free pixels, this significantly reduced usable pixels in cloudy regions. Future model iterations will aim to

© 2025 The Author(s). *Remote Sensing in Ecology and Conservation* published by John Wiley & Sons Ltd on behalf of Zoological Society of London.

20563485, 0, Downloaded from https://zslpublications.onlinelibrary.wiley.com/doi/10.1002/rse2.70041, Wiley Online Library on [01/03/2026]. See the Terms and Conditions (https://onlinelibrary.wiley.com/terms-and-conditions) on Wiley Online Library for rules of use; OA articles are governed by the applicable Creative Commons License

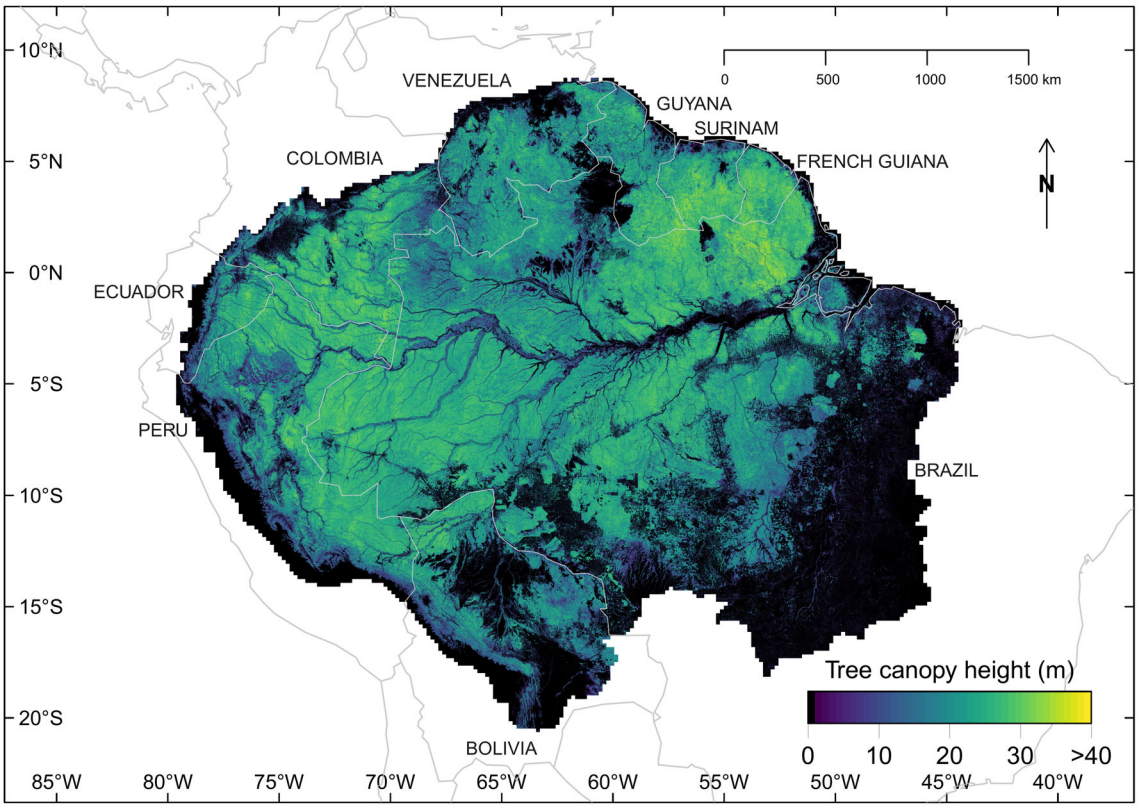

Figure 14. Canopy height of the Amazon forest (m). To facilitate visualization at very high resolution, the colors represent the estimates from our model, aggregated to an 80 m spatial resolution using the median.

predict heights under thin clouds to improve coverage and accuracy in Andean slopes. We also acknowledge that nearly all predictions outside Brazil are out-of-domain extrapolations, and independent assessments of CHM quality in these regions will be made as new LiDAR datasets emerge and are encouraged for those who have access to such data.

While rare Amazon trees can reach 65–88.5 m (Gorgens et al., 2019), our sample shows $\sim$ 20 m mean canopy height, with 22.1 m Amazon-wide average. GEDI data show canopy heights $>$ 40 m represent 5% in Amazon, 10% in African, and $>$ 25% in Asian rainforests (Bourgoin et al., 2024). Southeast Asian *Dipterocarp* forests are tallest, with mean heights recorded for a forest of Borneo averaging 50 m with individuals up to 98 m (Shenkin et al., 2019). We acknowledge that our model cannot currently capture these extremely tall trees and future work will incorporate other tropical forests to improve tall tree height estimation.

The intact Amazon offers a unique opportunity to study pristine tropical forests at scale. Our model could be used to locate all the giant trees in the Amazon forest (Fig. 15), which are crucial for biodiversity and ecosystem function (Enquist et al., 2020; Francis & Asner, 2019; Piirto & Rogers, 2002), to plan their protection against near-future risks. The high-resolution canopy height maps produced in this study could also be used as input for models estimating forest carbon stocks, as tree height is linked to aboveground biomass and carbon storage (Asner & Mascaro, 2014; Saatchi et al., 2011). Our height map also provides unprecedented canopy structure data where LiDAR is unavailable, which could inform on biodiversity to some extent, as forest structure and canopy height are indicators of habitat complexity and can be associated with species diversity (Enquist et al., 2020; Martins et al., 2017; Moudrý et al., 2024; Roll et al., 2015). Furthermore, our map could serve as a benchmark for monitoring forest degradation in the future, enabling the detection of height changes within the canopy at the tree level (Fig. 8) that might not be apparent in lower resolution height maps based on Landsat or Sentinel images.

Advances in canopy height changes mapping

Currently, tropical forest cover changes from deforestation, degradation, or regeneration at a regional to global

© 2025 The Author(s). *Remote Sensing in Ecology and Conservation* published by John Wiley & Sons Ltd on behalf of Zoological Society of London.

20563485, 0, Downloaded from https://zslpublications.onlinelibrary.wiley.com/doi/10.1002/rse2.70041, Wiley Online Library on [01/03/2026]. See the Terms and Conditions (https://onlinelibrary.wiley.com/terms-and-conditions) on Wiley Online Library for rules of use; OA articles are governed by the applicable Creative Commons License

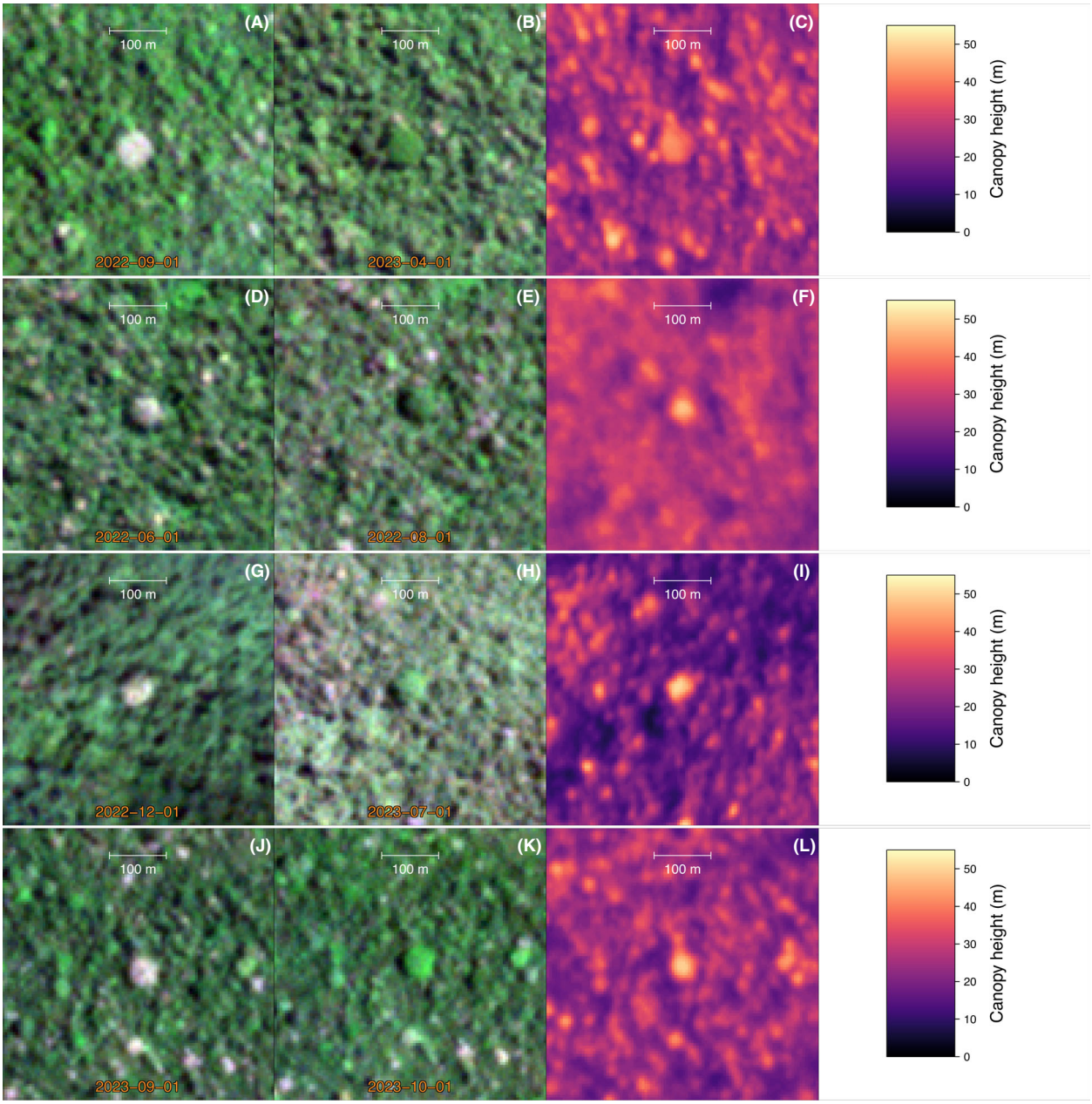

Figure 15. Examples of giant trees identified by our Amazon canopy height model. For each individual tree (row), a Planet NICFI image is shown during its leafless period (first column), during its leaf-covered period (second column), and the third column presents our canopy height composite for the year 2020. The resolution of the NICFI image, preserved in this figure, is 4.78 m. Tree coordinates in decimal latitude and longitude [−10.6957146, −67.03241]; [0.2214842, −75.18744]; [6.4737808, −61.35848]; and [−7.6873982, −68.93119].

scale are mostly made based on the semantic segmentation and time series analysis of classified pixels (Csillik et al., 2019; Dalagnol et al., 2023; Hansen et al., 2013; Heinrich et al., 2021, 2023; MapBiomas, 2024; Wagner et al., 2023). In regrowth analysis, the algorithm relies on forest cover classification rather than canopy height. For example, if a pasture becomes classified as forest and remains so for 10 years, the pixel is considered a 10-year regenerating secondary forest (Heinrich et al., 2021). This works well for regrowth after large tree cover removal or initially non-forested pixels, but logged or degraded pixels can lose height while remaining classified as unchanged forest cover. The canopy height could help in this case, but the remote sensing community is just beginning to

© 2025 The Author(s). *Remote Sensing in Ecology and Conservation* published by John Wiley & Sons Ltd on behalf of Zoological Society of London.

20563485, 0, Downloaded from https://zslpublications.onlinelibrary.wiley.com/doi/10.1002/rse2.70041, Wiley Online Library on [01/03/2026]. See the Terms and Conditions (https://onlinelibrary.wiley.com/terms-and-conditions) on Wiley Online Library for rules of use; OA articles are governed by the applicable Creative Commons License

map tropical forest cover changes using height. Most recent works on multitemporal height estimation use LiDAR data because open global canopy height products only contain a single date (Lang et al., 2023; Pauls et al., 2024; Potapov et al., 2021; Tolan et al., 2024). In the Amazon Arc of Deforestation, repeated LiDAR measurements demonstrated that forest height losses, carbon changes and growth from both anthropogenic and natural processes could be identified and estimated (Csillik et al., 2024). Similar datasets revealed dynamics of gap formation and closure, including tree growth in gaps (Dalagnol et al., 2021; Winstanley et al., 2024). Currently, only Planet's commercial Forest Carbon Monitoring (FCM) product provides global quarterly updates at 3 m resolution for canopy cover, height and aboveground carbon, though it remains non-peer-reviewed.

In this work, we demonstrate Planet NICFI time series' potential for mapping high-resolution canopy height changes, Figures 8 and 9. Our model captures logging activities and their impact on forest canopy height, Fig. 8. Despite some noise and phenology-related changes outside logging areas, detecting height decreases is promising, as such disturbances are extremely difficult to estimate from optical remote sensing. While locating activities like selective logging or fire impacts is currently possible (Dalagnol et al., 2023), quantifying height and biomass changes remains challenging. High-frequency time data, such as monthly Planet NICFI are crucial for tree loss detection, as tropical forest gaps can close within months through lateral ingrowth, potentially masking tree loss (Dalagnol et al., 2021; Winstanley et al., 2024). Using height time series (Fig. 9), deforestation appears as height changes, matching previously identified deforestation dates from tree cover changes (Wagner et al., 2023). Forest-to-pasture conversion shows near-zero heights (Fig. 9 points 1–3), while regrowth cases show increasing heights (Fig. 9 points 4–5). Though growth detection requires years, secondary forest growth detection is promising. The height time series (Fig. 9, point 6) enabled tracking changes in tree height for a forest regrowing from abandoned pasture since 2016. While requiring further validation, these results suggest potential for measuring regrowth using open-access NICFI images, previously achievable only through repeated LiDAR or commercial data.

Implications for Ecology and Conservation

The Amazon forest, as one of the largest carbon pools in terrestrial ecosystems, is a key element of the global carbon cycle and climate regulation (Lv et al., 2021; Mo et al., 2023; Pan et al., 2024; Rosan et al., 2024), and mapping its biomass remains a major challenge. Our map alone cannot be directly converted into biomass estimates, as additional parameters on the vertical distribution of vegetation would be needed (Longo et al., 2016). However, it can provide information for classifying forests by height and structural attributes, which may serve as proxies for biomass. As our map provides the finest detail of canopy height over the Amazon so far, it becomes possible to identify forests based on their canopy height characteristics and target them for sampling of biodiversity and biomass. In some cases, the canopy height characteristics alone may also justify considering certain forests for protection, for example, the Amazon's tallest forests in the Amapá region of Brazil.

Our model is the first that can estimate heights above 45 m in the Amazon forest, Figure 3. Furthermore, the largest individual trees are clearly visible in the predicted CHM, Figures 5, 6 and 15. While the tree crowns can be observed in RGB images, they are further enhanced in the canopy height visualizations, allowing the larger and tallest individuals to be visually identified, Figure 15. For example, visually locating the giant trees, each located in a different country (Fig. 15), required less than 2 h. Our map could be used to locate the largest individuals and the tallest forest of the Amazon forest which is of primary conservation importance, as large trees, being part of the megabiota, are more susceptible to extinction, and changes in their abundance disproportionately affect ecosystem and Earth system processes, including biomass, carbon, nutrients and fertility (Enquist et al., 2020).

In the Amazon, managed forest use mainly involves selective logging, which does not remove the entire canopy cover but only selected stems, and illegal logging (aside from clear-cut) tends to follow the same practice, where only a few stems are removed while the forest cover remains. Currently, there is no satellite-based data sufficiently accurate or with sufficient spatial coverage to detect the (illegal or legal) removal of individual trees. It is only currently made using LiDAR data (Csillik et al., 2024; Dalagnol et al., 2021; Longo et al., 2016) or VHR images (Dalagnol et al., 2019). Here, we show that just by taking the raw difference in predicted height between two dates, the locations of removed individual crowns could be observed, Figure 8, which suggests that the detection of individual tree removal by logging is feasible. In further work, we will analyze the changes detected by our approach, which will require validation with LiDAR data and temporal filtering or annual aggregation to remove noise from illumination, phenology and geolocation errors.

The restoration of tropical forests is considered one of the most effective strategies for climate change mitigation (Bastin et al., 2019; Hasler et al., 2024). However, there is currently no widely established model to monitor forest

© 2025 The Author(s). *Remote Sensing in Ecology and Conservation* published by John Wiley & Sons Ltd on behalf of Zoological Society of London.

20563485, 0, Downloaded from https://zslpublications.onlinelibrary.wiley.com/doi/10.1002/rse2.70041, Wiley Online Library on [01/03/2026]. See the Terms and Conditions (https://onlinelibrary.wiley.com/terms-and-conditions) on Wiley Online Library for rules of use; OA articles are governed by the applicable Creative Commons License

regrowth, and remote sensing methods for this purpose are still under development. To the best of our knowledge, only two studies have applied deep learning to measure forest regrowth (Schwartz et al., 2025; Wagner et al., 2025). While not validated with LiDAR, we show here that our algorithm was able to detect growth in height in a regenerating forest, Figure 9. In a recent study motivated by this observation, we applied the model developed in this work to *Pinus* and *Eucalyptus* plantations from 0 to 8 years in Southwest Brazil, where we also had LiDAR measurements (Wagner et al., 2025) and found that it can accurately track the regrowth of *Pinus* and, to a lesser extent, *Eucalyptus*, but yielding promising results for natural forest monitoring. In future work, we plan to explore and validate the application of the model to tropical forest regrowth, aiming to develop robust methods for large-scale monitoring of forest restoration.

Finally, the Amazon forest structure is diverse, and the LiDAR sample currently available does not yet capture the full range of ecosystems, such as the bamboo-dominated forests in Acre, the giant tree forests in Amapá, or areas with fertile soils influenced by the Andes, nor the large-scale nutrient and elevation gradients present across the basin (Asner et al., 2014; Dalagnol et al., 2018; Gorgens et al., 2019, 2021; Malhi et al., 2006; Quesada et al., 2012). Future work could examine whether these ecosystems or gradients are detectable in our map to further improve knowledge of domain-scale variation in height and biomass, and if not, investigate the underlying reasons to guide further improvements of the map.

Open data of canopy height

Our dataset is the first to enable the visualization of all the largest tree crowns in the Amazon. This raises questions regarding open data, as sharing such datasets could impact the surrounding communities and environments (Bennett et al., 2024). These large trees may be located on indigenous lands, areas with uncontacted people, or public/private lands. Public knowledge of their locations could attract scientific research, tourism, or logging, with unclear benefits or harms. While many large trees remain protected by isolation in remote areas, others near deforestation may only be known to loggers. Logging industries can access this information through aerial surveys or field exploration, but these trees remain unknown to local communities, governments, conservationists and tourism operators who could protect and sustainably use them. These trees could be fully protected or, if used in sustainable eco-tourism, could contribute to socio-bioeconomies (SBEs) (Garrett et al., 2024), defined as economies based on the sustainable use and restoration of Amazonian ecosystems, as well as Indigenous and rural livelihoods in the region.

A potential solution could involve developing a monitoring system to raise awareness about these trees, thereby increasing their protection by making their existence more visible to actors other than the loggers. As more people become aware, these trees, rather than being at greater risk, could actually benefit from the attention and protection brought about by public visibility, in an analogy to the use of public space in cities (Jacobs, 1961). Following the demand of the Remote Sensing community and experts, our dataset has been made available on AWS Open Data Registry (https://registry.opendata.aws/ctrees-amazon-canopy-height/), and in the Awesome Google Earth Engine (GEE) Community Catalog (https://gee-community-catalog.org/projects/ctrees_amazon/).

Conclusion

We present the first complete Amazon canopy height map at 4.78 m resolution (2020–2024), generated using a U-Net model trained on Planet NICFI imagery and airborne LiDAR data. We demonstrate that a U-Net model trained locally with high-quality LiDAR–Planet pairs provides reliable canopy height estimates at fine spatial resolution, with our model outperforming existing global products from Sentinel-2/1 and Maxar Vivid2. Our model is the only one able to capture heights above 45 m, and the resulting Amazon map captures key structural patterns, from the tallest trees in the Guiana Shield to shorter vegetation along wetlands, rivers, rocky outcrops, savannas and high elevations. Finally, we show that this resolution enables, to a certain extent, the detection of small-scale canopy height changes associated with deforestation, logging and regeneration, making it a potential new resource for monitoring forest structure across the Amazon.

Acknowledgments

The authors wish to thank the Grantham Foundation and High Tide Foundation for their generous gift to UCLA and support to CTrees.org. Part of this work was carried out at the Jet Propulsion Laboratory, California Institute of Technology, under a contract with the National Aeronautics and Space Administration (NASA).

Author Contributions

Fabien H Wagner: Conceptualization; methodology; software; data curation; investigation; validation; formal analysis; visualization; writing – original draft. **Ricardo Dalagnol:** Conceptualization; methodology; software;

© 2025 The Author(s). *Remote Sensing in Ecology and Conservation* published by John Wiley & Sons Ltd on behalf of Zoological Society of London.

20563485, 0, Downloaded from https://zslpublications.onlinelibrary.wiley.com/doi/10.1002/rse2.70041, Wiley Online Library on [01/03/2026]. See the Terms and Conditions (https://onlinelibrary.wiley.com/terms-and-conditions) on Wiley Online Library for rules of use; OA articles are governed by the applicable Creative Commons License

investigation; writing – review and editing. **Griffin Carter:** Conceptualization; methodology; software; investigation; writing – review and editing. **Mayumi C. M. Hirye:** Methodology; software; investigation; visualization; data curation; writing – review and editing. **Shivraj Gill:** Methodology; software; formal analysis; investigation; data curation; writing – review and editing. **Le Bienfaiteur Sagang Takougoum:** Validation; investigation; data curation; writing – review and editing. **Samuel Favrichon:** Conceptualization; methodology; software; investigation; writing – review and editing. **Michael Keller:** Data curation; writing – review and editing. **Jean P. H. B. Ometto:** Data curation; writing – review and editing. **Lorena Alves:** Writing – review and editing. **Cynthia Creze:** Writing – review and editing. **Stephanie P. George-Chacon:** Writing – review and editing. **Shuang Li:** Writing – review and editing. **Zhihua Liu:** Writing – review and editing. **Adugna Mullissa:** Writing – review and editing. **Yan Yang:** Writing – review and editing. **Erone G. Santos:** Writing – review and editing. **Sarah R. Worden:** Writing – review and editing. **Martin Brandt:** Writing – review and editing. **Philippe Ciais:** Writing – review and editing. **Stephen C. Hagen:** Writing – review and editing; project administration; funding acquisition; resources. **Sassan Saatchi:** Writing – review and editing; project administration; supervision; conceptualization; investigation; resources; funding acquisition.

Data Availability Statement

Our Amazon canopy height dataset is available on AWS Open Data Registry at https://registry.opendata.aws/ctrees-amazon-canopy-height/, and in the Awesome Google Earth Engine (GEE) Community Catalog at https://gee-community-catalog.org/projects/ctrees_amazon/. At the time of the study, Planetscope imagery in tropical areas via Norway's International Climate and Forest Initiative (NICFI) was available for non-commercial purposes from Planet Labs. It is now only available commercially from the Planet tropical forest observatory https://www.planet.com/tropical-forest-observatory/. The LiDAR datasets from the "Sustainable Landscapes – Brazil" are publicly available at https://daac.ornl.gov/CMS/guides/LiDAR_Forest_Inventory_Brazil.html and https://www.paisagenslidar.cnptia.embrapa.br/. Data and metadata of the EBA (Biomass Estimation of the Amazon) project LiDAR transects across the Brazilian Amazon are publicly available from https://zenodo.org/records/7636454 and https://zenodo.org/records/4968706. The LiDAR dataset covering the São Paulo Metropolitan Region (SPMR) is publicly available and distributed in LAZ files at https://registry.opendata.aws/pmsp-lidar/.

References

Abadi, M., Agarwal, A., Barham, P., Brevdo, E., Chen, Z., Citro, C., Corrado, G.S., Davis, A., Dean, J., Devin, M., Ghemawat, S., Goodfellow, I., Harp, A., Irving, G., Isard, M., Jia, Y., Jozefowicz, R., Kaiser, L., Kudlur, M., Levenberg, J., Mané, D., Monga, R., Moore, S., Murray, D., Olah, C., Schuster, M., Shlens, J., Steiner, B., Sutskever, I., Talwar, K., Tucker, P., Vanhoucke, V., Vasudevan, V., Viégas, F., Vinyals, O., Warden, P., Wattenberg, M., Wicke, M., Yu, Y., Zheng, X., 2015. TensorFlow: Large-scale machine learning on heterogeneous systems. https://www.tensorflow.org/.

Allaire, J., Chollet, F., 2016. keras: R Interface to 'Keras'. r package version 2.1.4. https://keras.rstudio.com.

Allaire, J., Tang, Y., 2020. tensorflow: R Interface to 'TensorFlow'. r package version 2.2.0. https://CRAN.R-project.org/package=tensorflow.

Asner, G.P., Anderson, C.B., Martin, R.E., Knapp, D.E., Tupayachi, R., Sinca, F. et al. (2014) Landscape-scale changes in forest structure and functional traits along an andes-to-amazon elevation gradient. *Biogeosciences*, **11**, 843–856. https://doi.org/10.5194/bg-11-843-2014

Asner, G.P. & Mascaro, J. (2014) Mapping tropical forest carbon: calibrating plot estimates to a simple lidar metric. *Remote Sensing of Environment*, **140**, 614–624.

Astola, H., Seitsonen, L., Halme, E., Molinier, M. & Lönnqvist, A. (2021) Deep neural networks with transfer learning for forest variable estimation using sentinel-2 imagery in boreal forest. *Remote Sensing*, **13**, 2392.

Avitabile, V., Herold, M., Heuvelink, G.B., Lewis, S.L., Phillips, O.L., Asner, G.P. et al. (2016) An integrated pan-tropical biomass map using multiple reference datasets. *Global Change Biology*, **22**, 1406–1420.

Bastin, J.F., Finegold, Y., Garcia, C., Mollicone, D., Rezende, M., Routh, D. et al. (2019) The global tree restoration potential. *Science*, **365**, 76–79.

Bennett, M.M., Gleason, C.J., Tellman, B., Alvarez Leon, L.F., Friedrich, H.K., Ovienmhada, U. et al. (2024) Bringing satellites down to earth: six steps to more ethical remote sensing. *Global Environmental Change Advances*, **2**, 100003. https://doi.org/10.1016/j.gecadv.2023.100003

Bourgoin, C., Ceccherini, G., Girardello, M., Vancutsem, C., Avitabile, V., Beck, P. et al. (2024) Human degradation of tropical moist forests is greater than previously estimated. *Nature*, **631**, 1–7.

Carter, G., Wagner, F.H., Dalagnol, R., Roberts, S., Ritz, A.L. & Saatchi, S. (2024) Detection of forest disturbance across california using deep-learning on planetscope imagery. *Frontiers in Remote Sensing*, **5**, 1409400.

Chollet F. 2015 Keras. https://keras.io

Csillik, O., Keller, M., Longo, M., Ferraz, A., Rangel Pinagé, E., Görgens, E.B. et al. (2024) A large net carbon loss attributed to anthropogenic and natural disturbances in the amazon

© 2025 The Author(s). *Remote Sensing in Ecology and Conservation* published by John Wiley & Sons Ltd on behalf of Zoological Society of London.

20563485, 0, Downloaded from https://zslpublications.onlinelibrary.wiley.com/doi/10.1002/rse2.70041, Wiley Online Library on [01/03/2026]. See the Terms and Conditions (https://onlinelibrary.wiley.com/terms-and-conditions) on Wiley Online Library for rules of use; OA articles are governed by the applicable Creative Commons License

arc of deforestation. *Proceedings of the National Academy of Sciences*, **121**, e2310157121.

Csillik, O., Kumar, P., Mascaro, J., O'Shea, T. & Asner, G.P. (2019) Monitoring tropical forest carbon stocks and emissions using planet satellite data. *Scientific Reports*, **9**, 1–12.

CTrees.org, 2024. Redd+ai: Tree cover loss and degradation from logging, fire and roads in tropical forests – v 1.0. https://ctrees.org/reddai.

da Silva, S.S., Brown, F., de Oliveira Sampaio, A., Silva, A.L.C., dos Santos, N.C.R.S., Lima, A.C. et al. (2023) Amazon climate extremes: increasing droughts and floods in Brazil's state of acre. *Perspectives in Ecology and Conservation*, **21**, 311–317.

Dalagnol, R., Phillips, O.L., Gloor, E., Galvão, L.S., Wagner, F.H., Locks, C.J. et al. (2019) Quantifying canopy tree loss and gap recovery in tropical forests under low-intensity logging using vhr satellite imagery and airborne lidar. *Remote Sensing*, **11**, 817.

Dalagnol, R., Wagner, F.H., Galvão, L.S., Braga, D., Osborn, F., da Conceição Bispo, P. et al. (2023) Mapping tropical forest degradation with deep learning and planet nicfi data. *Remote Sensing of Environment*, **298**, 113798.

Dalagnol, R., Wagner, F.H., Galvão, L.S., Nelson, B.W. & Aragão, L.E.O.e.C.d. (2018) Life cycle of bamboo in the southwestern amazon and its relation to fire events. *Biogeosciences*, **15**, 6087–6104.

Dalagnol, R., Wagner, F.H., Galvão, L.S., Streher, A.S., Phillips, O.L., Gloor, E. et al. (2021) Large-scale variations in the dynamics of amazon forest canopy gaps from airborne lidar data and opportunities for tree mortality estimates. *Scientific Reports*, **11**, 1–14.

de Almeida, C.A., Maurano, L.E.P., de Morisson Valeriano, D., Camara, G., Vinhas, L., Gomes, A.R., Monteiro, A.M.V., de Almeida Souza, A.A., Rennó, C.D., Silva, D.E. et al 2021. Methodology for forest monitoring used in prodes and deter projects. CEP 12, 010.

de Conto, T., Armston, J. & Dubayah, R. (2024) Characterizing the structural complexity of the earth's forests with spaceborne lidar. *Nature Communications*, **15** (1), 8116. https://doi.org/10.1038/s41467-024-52468-2

Dos-Santos, M., Keller, M., Pinage, E., Morton, D., 2022. Forest inventory and biophysical measurements, Brazilian Amazon, 2009–2018. ORNL DAAC.

Dubayah, R., Blair, J.B., Goetz, S., Fatoyinbo, L., Hansen, M., Healey, S. et al. (2020) The global ecosystem dynamics investigation: high-resolution laser ranging of the earth's forests and topography. *Science of Remote Sensing*, **1**, 100002.

Enquist, B.J., Abraham, A.J., Harfoot, M.B., Malhi, Y. & Doughty, C.E. (2020) The megabiota are disproportionately important for biosphere functioning. *Nature Communications*, **11**, 699.

FAO. (2020) *Global Forest Resources Assessment 2020: Main report*. Technical Report. ROME: Food and Agriculture Organization of the United Nations. https://doi.org/10.4060/ca9825en

Fayad, I., Ciais, P., Schwartz, M., Wigneron, J.P., Baghdadi, N., de Truchis, A., d'Aspremont, A., Frappart, F., Saatchi, S., Pellissier-Tanon, A., Bazzi, H., 2023. Vision transformers, a new approach for high-resolution and large-scale mapping of canopy heights. arXiv:2304.11487.

Feldpausch, T.R., Banin, L., Phillips, O.L., Baker, T.R., Lewis, S.L., Quesada, C.A. et al. (2011) Height-diameter allometry of tropical forest trees. *Biogeosciences*, **8**, 1081–1106.

Francis, E.J. & Asner, G.P. (2019) High-resolution mapping of redwood (sequoia sempervirens) distributions in three Californian forests. *Remote Sensing*, **11**, 1–19. https://doi.org/10.3390/rs11030351

Garrett, R., Ferreira, J., Abramovay, R., Brandão, J., Brondizio, E., Euler, A. et al. (2024) Transformative changes are needed to support socio-bioeconomies for people and ecosystems in the amazon. *Nature Ecology & Evolution*, **8**(10), 1815–1825. https://doi.org/10.1038/s41559-024-02467-9

GDAL/OGR Contributors. (2019) *GDAL/OGR Geospatial Data Abstraction software Library*. Open Source Geospatial Foundation. https://gdal.org

Ge, S., Gu, H., Su, W., Praks, J. & Antropov, O. (2022) Improved semisupervised unet deep learning model for forest height mapping with satellite sar and optical data. *IEEE Journal of Selected Topics in Applied Earth Observations and Remote Sensing*, **15**, 5776–5787.

Gloor, M., Brienen, R.J., Galbraith, D., Feldpausch, T.R., Schöngart, J., Guyot, J.L. et al. (2013) Intensification of the amazon hydrological cycle over the last two decades. *Geophysical Research Letters*, **40**, 1729–1733.

Gonçalves, N.B., Rosa, D.M., do Valle, D.F., Smith, M.N., Dalagnol, R., de Almeida, D.R.A. et al. (2024) Revealing forest structural "fingerprints": an integration of lidar and deep learning uncovers topographical influences on central amazon forests. *Ecological Informatics*, **81**, 102628. https://doi.org/10.1016/j.ecoinf.2024.102628

Gorgens, E.B., Motta, A.Z., Assis, M., Nunes, M.H., Jackson, T., Coomes, D. et al. (2019) The giant trees of the amazon basin. *Frontiers in Ecology and the Environment*, **17**, 373–374.

Gorgens, E.B., Nunes, M.H., Jackson, T., Coomes, D., Keller, M., Reis, C.R. et al. (2021) Resource availability and disturbance shape maximum tree height across the amazon. *Global Change Biology*, **27**, 177–189.

Hansen, M.C., Potapov, P.V., Moore, R., Hancher, M., Turubanova, S.A., Tyukavina, A. et al. (2013) High-resolution global maps of 21st-century forest cover change. *Science*, **342**(6160), 850–853. https://doi.org/10.1126/science.1244693

Hasler, N., Williams, C.A., Denney, V.C., Ellis, P.W., Shrestha, S., Terasaki Hart, D.E. et al. (2024) Accounting for albedo

© 2025 The Author(s). *Remote Sensing in Ecology and Conservation* published by John Wiley & Sons Ltd on behalf of Zoological Society of London.

20563485, 0, Downloaded from https://zslpublications.onlinelibrary.wiley.com/doi/10.1002/rse2.70041, Wiley Online Library on [01/03/2026]. See the Terms and Conditions (https://onlinelibrary.wiley.com/terms-and-conditions) on Wiley Online Library for rules of use; OA articles are governed by the applicable Creative Commons License

change to identify climate-positive tree cover restoration. *Nature Communications*, **15**, 2275.
Heinrich, V.H., Dalagnol, R., Cassol, H.L., Rosan, T.M., de Almeida, C.T., Silva Junior, C.H. et al. (2021) Large carbon sink potential of secondary forests in the brazilian amazon to mitigate climate change. *Nature Communications*, **12**, 1–11.
Heinrich, V.H., Vancutsem, C., Dalagnol, R., Rosan, T.M., Fawcett, D., Silva-Junior, C.H. et al. (2023) The carbon sink of secondary and degraded humid tropical forests. *Nature*, **615**, 436–442.
Huang, D., Tang, Y. & Qin, R. (2022) An evaluation of planetscope images for 3d reconstruction and change detection–experimental validations with case studies. *GIScience & Remote Sensing*, **59**, 744–761.
Hubbell, S.P., He, F., Condit, R., Borda-de Água, L., Kellner, J. & Ter Steege, H. (2008) How many tree species are there in the amazon and how many of them will go extinct? *Proceedings of the National Academy of Sciences*, **105**, 11498–11504.
Illarionova, S., Shadrin, D., Ignatiev, V., Shayakhmetov, S., Trekin, A. & Oseledets, I. (2022) Estimation of the canopy height model from multispectral satellite imagery with convolutional neural networks. *IEEE Access*, **10**, 34116–34132.
Jacobs, J. (1961) *The death and life of great American cities*. New York: Random House Inc.
Karatsiolis, S., Kamilaris, A. & Cole, I. (2021) Img2ndsm: height estimation from single airborne rgb images with deep learning. *Remote Sensing*, **13**, 2417.
Kattenborn, T., Leitloff, J., Schiefer, F. & Hinz, S. (2021) Review on convolutional neural networks (cnn) in vegetation remote sensing. *ISPRS Journal of Photogrammetry and Remote Sensing*, **173**, 24–49. https://doi.org/10.1016/j.isprsjprs.2020.12.010
Lang, N., Jetz, W., Schindler, K. & Wegner, J.D. (2023) A high-resolution canopy height model of the earth. *Nature Ecology & Evolution*, **7**, 1778–1789.
Lang, N., Schindler, K. & Wegner, J.D. (2019) Country-wide high-resolution vegetation height mapping with sentinel-2. *Remote Sensing of Environment*, **233**, 111347.
Lapola, D., Pinho, P., Barlow, J., Aragão, L., Berenguer, E., Carmenta, R. et al. (2023) The drivers and impacts of amazon forest degradation. *Science*, **379**, eabp8622.
Laurance, W.F., Fearnside, P.M., Laurance, S.G., Delamonica, P., Lovejoy, T.E., Rankin-de Merona, J.M. et al. (1999) Relationship between soils and amazon forest biomass: a landscape-scale study. *Forest Ecology and Management*, **118**, 127–138.
Lefsky, M.A. (2010) A global forest canopy height map from the moderate resolution imaging spectroradiometer and the geoscience laser altimeter system. *Geophysical Research Letters*, **37**, 1–5.
Lefsky, M.A., Harding, D.J., Keller, M., Cohen, W.B., Carabajal, C.C., Del Bom Espirito-Santo, F. et al. (2005) Estimates of forest canopy height and aboveground biomass using icesat. *Geophysical Research Letters*, **32**, 1–4.
Li, S., Brandt, M., Fensholt, R., Kariryaa, A., Igel, C., Gieseke, F. et al. (2023) Deep learning enables image-based tree counting, crown segmentation, and height prediction at national scale. *PNAS Nexus*, **2**, pgad076. https://doi.org/10.1093/pnasnexus/pgad076
Li, X., Wang, M. & Fang, Y. (2020) Height estimation from single aerial images using a deep ordinal regression network. *IEEE Geoscience and Remote Sensing Letters*, **19**, 1–5.
Lim, K., Treitz, P., Wulder, M., St-Onge, B. & Flood, M. (2003) Lidar remote sensing of forest structure. *Progress in Physical Geography*, **27**, 88–106.
Liu, S., Brandt, M., Nord-Larsen, T., Chave, J., Reiner, F., Lang, N., Tong, X., Ciais, P., Igel, C., Li1, S., Mugabowindekwe, M., Saatchi, S., Yue, Y., Chen, Z., Fensholt, R., 2023. The overlooked contribution of trees outside forests to tree cover and woody biomass across europe. Preprint (Version 1). Research Square. https://doi.org/10.21203/rs.3.rs-2573442/v1.
Liu, S., Csillik, O., Ordway, E.M., Chang, L.L., Longo, M., Keller, M. et al. (2025) Environmental drivers of spatial variation in tropical forest canopy height: insights from Nasa's gedi spaceborne lidar. *Proceedings of the National Academy of Sciences of the United States of America*, **122**, e2401755122.
Longo, M., Keller, M., dos Santos, M.N., Leitold, V., Pinagé, E.R., Baccini, A. et al. (2016) Aboveground biomass variability across intact and degraded forests in the brazilian amazon. *Global Biogeochemical Cycles*, **30**, 1639–1660.
Luize, B.G., Tuomisto, H., Ekelschot, R., Dexter, K.G., Amaral, I.L.d., Coelho, L.d.S. et al. (2024) The biogeography of the amazonian tree flora. *Communications Biology*, **7**, 1240.
Lv G. J M. Ls B. N R.C. Ap A. 2021 Science panel for the Amazon. Cross-Chapter–The Amazon Carbon Budget 4
Malhi, Y., Wood, D., Baker, T.R., Wright, J., Phillips, O.L., Cochrane, T. et al. (2006) The regional variation of aboveground live biomass in old-growth amazonian forests. *Global Change Biology*, **12**, 1107–1138.
MapBiomas. (2024) *Project MapBiomas, Collection 8.0 of Brazilian Land Cover & Use Map Series*. Technical Report. MapBiomas. https://brasil.mapbiomas.org/colecoes-mapbiomas/
Marengo, J.A. & Espinoza, J.C. (2016) Extreme seasonal droughts and floods in amazonia: causes, trends and impacts. *International Journal of Climatology*, **36**, 1033–1050.
Markus, T., Neumann, T., Martino, A., Abdalati, W., Brunt, K., Csatho, B. et al. (2017) The ice, cloud, and land elevation satellite-2 (icesat-2): science requirements, concept, and implementation. *Remote Sensing of Environment*, **190**, 260–273.

© 2025 The Author(s). *Remote Sensing in Ecology and Conservation* published by John Wiley & Sons Ltd on behalf of Zoological Society of London.

20563485, 0, Downloaded from https://zslpublications.onlinelibrary.wiley.com/doi/10.1002/rse2.70041, Wiley Online Library on [01/03/2026]. See the Terms and Conditions (https://onlinelibrary.wiley.com/terms-and-conditions) on Wiley Online Library for rules of use; OA articles are governed by the applicable Creative Commons License

Martins, A.C., Willig, M.R., Presley, S.J. & Marinho-Filho, J. (2017) Effects of forest height and vertical complexity on abundance and biodiversity of bats in amazonia. *Forest Ecology and Management*, **391**, 427–435.

Matricardi, E.A.T., Skole, D.L., Costa, O.B., Pedlowski, M.A., Samek, J.H. & Miguel, E.P. (2020) Long-term forest degradation surpasses deforestation in the brazilian amazon. *Science*, **369**, 1378–1382.

Meta and World Resources Institute (WRI), 2023. High Resolution Canopy Height Maps by WRI and Meta. Meta and World Resources Institute (WRI) - 2023. High Resolution Canopy Height Maps (CHM). https://registry.opendata.aws/dataforgood-fb-forests

Mo, L., Zohner, C.M., Reich, P.B., Liang, J., De Miguel, S., Nabuurs, G.J. et al. (2023) Integrated global assessment of the natural forest carbon potential. *Nature*, **624**, 92–101.

Moudrý, V., Gábor, L., Marselis, S., Pracná, P., Barták, V., Prošek, J. et al. (2024) Comparison of three global canopy height maps and their applicability to biodiversity modeling: accuracy issues revealed. *Ecosphere*, **15**, e70026. https://doi.org/10.1002/ecs2.70026

National Institute for Space Research (INPE), Earth Observation General Coordination, 2024. Monitoring program of the Amazon and other biomes. Deforestation – legal Amazon. Technical Report. INPE. https://terrabrasilis.dpi.inpe.br/downloads/.

Ometto, J.P., Gorgens, E.B., de Souza Pereira, F.R., Sato, L., de Assis, M.L.R., Cantinho, R. et al. (2023) A biomass map of the Brazilian amazon from multisource remote sensing. *Scientific Data*, **10**, 668.

Pan, Y., Birdsey, R.A., Phillips, O.L., Houghton, R.A., Fang, J., Kauppi, P.E. et al. (2024) The enduring world forest carbon sink. *Nature*, **631**, 563–569.

Pauls, J., Zimmer, M., Kelly, U.M., Schwartz, M., Saatchi, S., Ciais, P., Pokutta, S., Brandt, M., Gieseke, F., 2024. Estimating canopy height at scale. arXiv:2406.01076.

Piirto, D.D. & Rogers, R.R. (2002) An ecological basis for managing giant sequoia ecosystems. *Environmental Management*, **30**, 110–128.

Planet Team 2017 Planet application program interface: In space for life on earth. https://api.planet.com

Pooja, P., Joe Kington, A.K. & Curdoglo, M. (2021) *Addendum to planet basemaps. Product specifications. Nicfi basemaps. v02*. San Francisco, California, USA: NICFI Basemaps.

Potapov, P., Li, X., Hernandez-Serna, A., Tyukavina, A., Hansen, M.C., Kommareddy, A. et al. (2021) Mapping global forest canopy height through integration of gedi and landsat data. *Remote Sensing of Environment*, **253**, 112165.

Qin, Y., Xiao, X., Wigneron, J.P., Ciais, P., Brandt, M., Fan, L. et al. (2021) Carbon loss from forest degradation exceeds that from deforestation in the brazilian amazon. *Nature Climate Change*, **11**, 442–448.

Quesada, C.A., Phillips, O.L., Schwarz, M., Czimczik, C.I., Baker, T.R., Patiño, S. et al. (2012) Basin-wide variations in amazon forest structure and function are mediated by both soils and climate. *Biogeosciences*, **9**, 2203–2246.

R Core Team. (2016) *R: A Language and Environment for Statistical Computing*. Vienna, Austria: R Foundation for Statistical Computing. https://www.R-project.org/

Rolf, E., Gordon, L., Tambe, M., Davies, A., 2024. Contrasting local and global modeling with machine learning and satellite data: a case study estimating tree canopy height in African savannas. arXiv preprint. arXiv:2411.14354.

Roll, U., Geffen, E. & Yom-Tov, Y. (2015) Linking vertebrate species richness to tree canopy height on a global scale. *Global Ecology and Biogeography*, **24**, 814–825.

Ronneberger, O., Fischer, P., Brox, T., 2015. U-net: convolutional networks for biomedical image segmentation. CoRR. arXiv:1505.04597. http://arxiv.org/abs/1505.04597.

Rosa, D., Nelson, B., Valle, D., Schietti, J., Almeida, D., Stark, S. et al. (2017) Forest structure gradient along a central amazon catena revealed by ground lidar. In: *Conference: Simpósio Brasileiro de Sensoriamento RemotoAt*, Brazil: Santos, SP, Vol. **XVIII**, pp. 2301–2306.

Rosan, T.M., Sitch, S., O'sullivan, M., Basso, L.S., Wilson, C., Silva, C. et al. (2024) Synthesis of the land carbon fluxes of the amazon region between 2010 and 2020. *Communications Earth & Environment*, **5**, 46.

Roussel, J.R., Auty, D., 2021. Airborne LiDAR Data Manipulation and Visualization for Forestry Applications. r package version 3.2.2. https://cran.r-project.org/package=lidR.

Roussel, J.R., Auty, D., Coops, N.C., Tompalski, P., Goodbody, T.R., Meador, A.S. et al. (2020) lidr: an r package for analysis of airborne laser scanning (als) data. *Remote Sensing of Environment*, **251**, 112061. https://doi.org/10.1016/j.rse.2020.112061

Saatchi, S.S., Harris, N.L., Brown, S., Lefsky, M., Mitchard, E.T., Salas, W. et al. (2011) Benchmark map of forest carbon stocks in tropical regions across three continents. *Proceedings of the National Academy of Sciences of the United States of America*, **108**, 9899–9904.

Schwartz, M., Ciais, P., De Truchis, A., Chave, J., Ottlé, C., Vega, C. et al. (2023) Forms: Forest multiple source height, wood volume, and biomass maps in France at 10 to 30 m resolution based on sentinel-1, sentinel-2, and global ecosystem dynamics investigation (gedi) data with a deep learning approach. *Earth System Science Data*, **15**, 4927–4945. https://doi.org/10.5194/essd-15-4927-2023

Schwartz, M., Ciais, P., Ottlé, C., De Truchis, A., Vega, C., Fayad, I. et al. (2024) High-resolution canopy height map in the landes forest (France) based on gedi, sentinel-1, and sentinel-2 data with a deep learning approach. *International Journal of Applied Earth Observation and Geoinformation*, **128**, 103711. https://doi.org/10.1016/j.jag.2024.103711

© 2025 The Author(s). *Remote Sensing in Ecology and Conservation* published by John Wiley & Sons Ltd on behalf of Zoological Society of London.

20563485, 0, Downloaded from https://zslpublications.onlinelibrary.wiley.com/doi/10.1002/rse2.70041, Wiley Online Library on [01/03/2026]. See the Terms and Conditions (https://onlinelibrary.wiley.com/terms-and-conditions) on Wiley Online Library for rules of use; OA articles are governed by the applicable Creative Commons License

Schwartz, M., Ciais, P., Sean, E., de Truchis, A., Vega, C., Besic, N. et al. (2025) Retrieving yearly forest growth from satellite data: a deep learning based approach. *Remote Sensing of Environment*, **330**, 114959. https://doi.org/10.1016/j.rse.2025.114959

Shenkin, A., Chandler, C.J., Boyd, D.S., Jackson, T., Disney, M., Majalap, N. et al. (2019) The world's tallest tropical tree in three dimensions. *Frontiers in Forests and Global Change*, **2**, 1–5. https://doi.org/10.3389/ffgc.2019.00032

Silva Junior, C.H., Heinrich, V.H., Freire, A.T., Broggio, I.S., Rosan, T.M., Doblas, J. et al. (2020) Benchmark maps of 33 years of secondary forest age for Brazil. *Scientific Data*, **7**, 269.

Skidmore, A.K., Coops, N.C., Neinavaz, E., Ali, A., Schaepman, M.E., Paganini, M. et al. (2021) Priority list of biodiversity metrics to observe from space. *Nature Ecology & Evolution*, **5**, 896–906.

Ter Steege, H., Pitman, N.C., Sabatier, D., Baraloto, C., Salomão, R.P., Guevara, J.E. et al. (2013) Hyperdominance in the amazonian tree flora. *Science*, **342**, 1243092.

Tolan, J., Yang, H.I., Nosarzewski, B., Couairon, G., Vo, H.V., Brandt, J. et al. (2024) Very high resolution canopy height maps from RGB imagery using self-supervised vision transformer and convolutional decoder trained on aerial lidar. *Remote Sensing of Environment*, **300**, 113888.

Wagner, F.H., Breunig, F.M., Balbinot, R., Silva, E.A., Soares, M.C., Kramm, M.A. et al. (2025) Monitoring the early growth of pinus and eucalyptus plantations using a planet nicfi-based canopy height model: a case study in riqueza, Brazil. *Remote Sensing*, **17**, 1–21. https://doi.org/10.3390/rs17152718

Wagner, F.H., Dalagnol, R., Silva-Junior, C.H.L., Carter, G., Ritz, A.L., Hirye, M.C.M. et al. (2023) Mapping tropical forest cover and deforestation with planet nicfi satellite images and deep learning in mato grosso state (Brazil) from 2015 to 2021. *Remote Sensing*, **15**, 1–21. https://doi.org/10.3390/rs15020521

Wagner, F.H., Roberts, S., Ritz, A.L., Carter, G., Dalagnol, R., Favrichon, S. et al. (2024) Sub-meter tree height mapping of california using aerial images and lidar-informed u-net model. *Remote Sensing of Environment*, **305**, 114099. https://doi.org/10.1016/j.rse.2024.114099

Winstanley, P., Dalagnol, R., Mendiratta, S., Braga, D., Galvão, L.S. & Bispo, P.d.C. (2024) Post-logging canopy gap dynamics and forest regeneration assessed using airborne lidar time series in the brazilian amazon with attribution to gap types and origins. *Remote Sensing*, **16**, 1–18. https://doi.org/10.3390/rs16132319

Zapata-Ríos, G., Andreazzi, C.S., Carnaval, A.C., da Costa Doria, C.R., Duponchelle, F., Flecker, A., Guayasamín, J.M., Heilpern, S., Jenkins, C.N., Maldonado, C. et al 2022. Chapter 3: Biological diversity and ecological networks in the amazon. https://www.theamazonwewant.org/amazon-assessment-report-2021/.

© 2025 The Author(s). *Remote Sensing in Ecology and Conservation* published by John Wiley & Sons Ltd on behalf of Zoological Society of London.

20563485, 0, Downloaded from https://zslpublications.onlinelibrary.wiley.com/doi/10.1002/rse2.70041, Wiley Online Library on [01/03/2026]. See the Terms and Conditions (https://onlinelibrary.wiley.com/terms-and-conditions) on Wiley Online Library for rules of use; OA articles are governed by the applicable Creative Commons License